Delft University of Technology
Faculty of Civil Engineering and Geosciences
MSc. Civil Engineering
Geotechnical Engineering

Characterizing the CPT response and particle size distribution of fluvially deposited Pleistocene sand in the Netherlands

Fenna van Aarle 4692756

Dr.ir. Dominique Ngan-Tillard
Ir. Kevin Duffy
Dr. Kay Koster
Dr. Joep Storms

Submission date: August 2, 2024

Abstract

Understanding the geological and geotechnical properties of the shallow subsurface is essential for making informed engineering decisions, especially in densely populated areas like the Netherlands. Urban areas are constructed on a complex mixture of sand, clay, loam, gravel, and organic materials that have accumulated over hundreds of thousands of years. Among these units is the Kreftenheye Formation, a fluvially deposited sand that is prevalent in the western part of the country and plays a critical role in foundation design and groundwater dynamics. The formation is therefore well described by geotechnical tests and geological tests, yet integrating both types of data has rarely been done on a nationwide scale.

This thesis addresses this gap by analyzing an extensive dataset provided by TNO – Geological Survey of the Netherlands, consisting of nearly 200 Cone Penetration Tests (CPT) paired with borehole data, generally reaching depths of up to 40 meters. The research employs a multi-faceted approach: a detailed local analysis examines layer transitions and CPT cone sensing distances, while a broader analysis of CPT data and grain size measurements identifies spatial and compositional patterns within the formation. Additionally, the thesis tests the Boulanger & DeJong (2018) filter method to assess its effectiveness in enhancing CPT data interpretation.

Key findings of this research highlight the impact of weak layers on CPT responses, emphasizing the need for careful consideration of the sensing and developmental distances of the CPT cone when interpreting results. The analysis reveals distinct geotechnical differences between northern and southern areas within the Kreftenheye Formation, with the southern area exhibiting coarser and more uniform sediments compared to the northern area. The study also addresses the challenges of distinguishing the Ockenburg Member from the undifferentiated Kreftenheye Formation using CPT data alone, due to their similar characteristics and overlapping data. Furthermore, the application of the Boulanger & DeJong (2018) filter method proves effective in refining data analysis and enhancing the robustness of the results.

Overall, this thesis contributes to a deeper understanding of the Kreftenheye Formation by integrating geological and geotechnical data, providing valuable insights for improved ground modeling and foundation design. The findings underscore the importance of a comprehensive approach in subsurface characterization and offer a foundation for future research in geotechnical and geological integration.

Contents

1 Introduction **6**

2 Literature Review **8**
2.1 Sand Overview 8
2.1.1 Geotechnical Relevance 8
2.1.2 Sand characteristics 9
2.1.3 Soil Deposition 13
2.1.4 Dutch Lithostratigraphic Units 18
2.2 Background on Testing Methods 19
2.2.1 Cone Penetration Test 19
2.2.2 Particle Size Analysis 25
2.3 Depositional History of the Kreftenheye Formation 25
2.3.1 Geological Time Frame 25
2.3.2 Members 27

3 Methods **33**
3.1 Database 33
3.1.1 General Description 33
3.1.2 Visualization and Validation 37
3.2 Boulanger and deJong (2014) CPT Filter method 44
3.2.1 Purpose and Use 44
3.2.2 Sensitivity 47

4 Results and Discussion **49**
4.1 General Kreftenheye Formation Analysis 49
4.2 Area A and B 53
4.3 Borehole Features and Local Geological Characteristics 56
4.3.1 Sensing distance Wijchen Bed 56
4.3.2 Weak zones within the Formation 57

5 Conclusion and Recommendations **59**

Bibliography **61**

List of Figures

2.1 Classification by roundness and sphericity of grains, from Krumbein (1941), modified by Ulusoy (2019) . . . 10
2.2 Schematic example of a grain size distribution plot from Zhang et al. (2018) . . 11
2.3 Sedimentary cycle of soils . . . 13
2.4 Example FFG, braided river (retrieved from: Science (2018)) . . . 16
2.5 Example FFZ, meandering river (retrieved from: Ecopedia (2024)) . . . 16
2.6 Example FFKLA, residual channel (retrieved from: Natuurkennis (2024)) . . . 16
2.7 Example FFKMA, floodplain (retrieved from: EOS (2023)) . . . 17
2.8 Example FFL, River bank (retrieved from: Gebiedsontwikkeling.nu (2023)) . . 17
2.9 Example FOVAM/FOVEU, marsh land (retrieved from: Geographic (2024)) . . 17
2.10 Geometry of the cone penetrometer from Robertson & Cabal (2014) . . . 19
2.11 Schematic overview of standard CPT corrections . . . 21
2.12 Texture-based classification system from Robertson (1990) . . . 22
2.13 Piezocone soil classification chart from Schneider et al. (2008) . . . 22
2.14 Behaviour based classification from Robertson (2016) . . . 23
2.15 Dutch Soil classification chart adapted from Robertson (1990) by FUGRO Ingenieursbureau B.V. (2010) . . . 23
2.16 Simplified paleogeographical maps of the Netherlands during the late Saalian, Eemian, and Weichselian periods. Adapted from Busschers et al. (2007) and Wong et al. (2007) . . . 26
2.17 Borehole B15F1501 in Rutten retrieved from TNO-GSN (2024) . . . 28
2.18 Borehole B30G4694 in Wassenaar retrieved from TNO-GSN (2024)) . . . 30
2.19 Borehole B37B3833 in s'Gravenzande retrieved from TNO-GSN (2024) . . . 31
2.20 Area A and B Kreftenheye Formation . . . 32

3.1 Map of the Netherlands showing the locations of the CPT and borehole pairs, including a subset of locations within the Kreftenheye Formation used in this study. . . . 34
3.2 Overview of the dataset of the Kreftenheye Formation used in this study. . . . 35
3.3 Map of the Netherlands showing the locations of the CPT and borehole pairs for the different members . . . 35
3.4 Overview of available data at one example location. Left pane: CPT measurements (CPT000000063319), left central panel: grain size measurements, central right panel: gravel content, right panel: borehole (B30E1024) lithology . . . 38
3.5 Schematic overview of combining CPT and borehole data - Layer selection . . 39

3.6 Schematic overview of combining CPT and borehole data - Sample selection. The dashed lines show the thickness of the sample and the blue highlighted line shows the selected CPT data 40
3.7 5 CPT measurements and grain size distributions within 6 kilometre distance (CPT000000018696, CPT000000018697, CPT000000018698, CPT000000018688, CPT000000018693) 41
3.8 3 CPT measurements and grain size distributions within 6 kilometre distance (CPT000000063319, CPT000000012728, CPT000000063320) 42
3.9 7 CPT and grain size distributions from West to East of the Netherlands (CPT000000080417, CPT000000050619, CPT000000012733, CPT000000012732, CPT000000012744, CPT000000012741, CPT000000063344) 43
3.10 7 CPT and grain size distributions from West to East of the Netherlands (CPT000000012728, CPT000000012751, CPT000000025396, CPT000000012737, CPT000000080414, CPT000000063329, CPT000000063332) 44
3.11 Thin layer effect (from Boulanger & DeJong (2018)) 45
3.12 Filter method weight function (from Boulanger & DeJong (2018)) 46
3.13 Sensitivity of m_z 47
3.14 Sensitivity of $z'_{50,ref}$ 48

4.1 Histogram of filtered q_c measurements and cumulative grain size distribution plot for the (undifferentiated) Kreftenheye Formation 50
4.2 Histogram of filtered q_c measurements and cumulative grain size distribution plot for the Zutphen Member 51
4.3 Histogram of filtered q_c measurements and cumulative grain size distribution plot for the Ockenburg Member 52
4.4 Histogram of filtered q_c measurements and cumulative grain size distribution plot for the Wijchen Member 53
4.5 Robertson (1990) soil classification chart and the cumulative grain size distribution for Areas A and B of the undifferentiated Kreftenheye Formation. 27 CPTs and 157 grain size distributions for Area A, 26 CPTs and 256 grain size distributions for Area B 54
4.6 Gravel Percentage of Area A and B 55
4.7 Autocorrelation functions 55
4.8 Influence of sensing distance on the Wijchen Bed. Left pane: photo taken from the borehole (B37E3413), central panel: CPT of the same interval (CPT000000012746), right panel: grainsize measurements for the interval 57
4.9 Intermediate soft layer within the Kreftenheye Formation. Left pane: photo taken from the borehole (B14E0952), central panel: CPT of the same interval (CPT000000043211), right panel: grainsize measurements for the interval . . . 58

List of Tables

2.1 Grain sizes from NEN 14688-1 (Netherlands Standardization Institute (2020)) . 10
2.2 Effects of transportation on sediments (Lambe & Whitman (1991)) 15

3.1 TopIntegraal locations 36
3.2 TopIntegraal grainsize data 36
3.3 TopIntegraal CPT data 37

4.1 Vertical scale of fluctuation 55

Chapter 1

Introduction

In the Netherlands, a fluvially deposited Pleistocene sand, knows as the Kreftenheye Formation, is widespread across the country and the Dutch North Sea Sector (Busschers et al. (2007); TNO-GSN (2024)). In the densely populated western areas of the country, the formation is typically overlain by clay and peat of Holocene age (Ngan-Tillard et al. (2010); Koster et al. (2018)). Consequently, most infrastructure and buildings in these areas are founded on piles. These foundation piles are driven through the overlying soft sediment, transferring the majority of the load to the stiff sand of the Kreftenheye Formation, which makes it an important geotechnical layer in the Dutch subsurface.

Nevertheless, the formation poses some engineering challenges as well. The Kreftenheye Formation is generally dense to very dense, with Cone Penetration Test (CPT) tip resistances reaching more than 80 MPa in some zones. Installing piles to their target depth whilst avoiding refusal and pile damage can therefore be challenging (de Gijt et al. (2019); Duffy et al. (2024)). Furthermore, weak zones within this layer can bring unexpected changes in the pile installation resistance and affect the ultimate bearing capacity of the pile.

Traditionally, many studies have tended to focus on the geological characterization of formations, often missing out on important patterns revealed by geotechnical data such as CPTs (Busschers et al. (2005); TNO-GSN (2024)). Conversely, CPT-focused research and industry practices may disregard the geological origin of deposits and overlook essential insights into the formation's history and potential risks (Robertson (2016); Mayne (2017)). By integrating both geological and geotechnical perspectives, a more comprehensive understanding of subsurface conditions can be achieved, leading to better-informed engineering decisions.

This thesis aims to address this integration challenge by presenting and analyzing a unique dataset of nearly 200 Cone Penetration Tests (CPT) and borehole pairs provided by TNO - Geological Survey of The Netherlands. This dataset includes detailed grain size measurements using a laser diffraction particle size analysis. The study focuses on the geotechnical and geological characteristics of the Kreftenheye Formation, with particular attention to how these factors influence geotechnical engineering design.

The structure of this thesis is designed to provide a comprehensive analysis of the Kreftenheye Formation through a detailed literature review, a methodology section, and an interpretation of the results. Chapter 2, the Literature Review, establishes foundational knowledge by discussing the geotechnical relevance of sands, their characteristics, deposition processes, and lithostratigraphy. This is followed by background information on the testing methods employed

to build the database. The third section of the literature review focuses on the depositional history of the Kreftenheye Formation, providing the geological context necessary for subsequent database analysis.

Chapter 3 outlines the methods used in the study, beginning with a detailed description of the dataset, including aspects of database visualization and validation. This is followed by an explanation of the Boulanger & DeJong (2018) filter method applied to the data.

The results and discussion Chapter 4 offers an in-depth analysis, starting with a general overview of the grain size measurements and CPT response of the Kreftenheye Formation. This analysis connects the geological findings from the literature review with the results of the data analysis. It continues with a detailed examination of the differences between Area A and Area B within the Kreftenheye Formation to enhance ground modeling. The section concludes with an exploration of local features observed in borehole and CPT measurements. This integrated approach combines geological and geotechnical insights to provide a deeper understanding of the Kreftenheye Formation.

The final Chapter 5 summarizes the key contributions of the research, highlights the benefits of integrating geological and geotechnical knowledge for engineering practice, and suggests potential directions for future research in this field.

Chapter 2

Literature Review

Understanding the Kreftenheye Formation through the analysis of the Cone Penetration Test (CPT) and borehole database requires a comprehensive background on several key topics. This literature review chapter aims to provide the foundational knowledge by exploring three main sections.

The first section, called Sand Overview, introduces all the essential information on sand within the Kreftenheye. It starts by showing the relevance of studying the Kreftenheye Formation within the field of geotechnical engineering. Then it delves into the characteristics of sand, discussing its grain and bulk properties. The section proceeds to examine the processes by which sand and other soils are deposited, offering insights into sedimentary environments. Additionally, it describes the basics of Dutch lithostratigraphy and reviews other significant formations in the Netherlands. This establishes a thorough understanding of the basic attributes of the Kreftenheye Formation.

The second section, Background on Testing Methods, focuses on the testing methods used to gather the database, specifically the Cone Penetration Test (CPT) and particle size analysis. It provides a detailed background on these techniques, explaining their principles, interpretation, uncertainties, and related prior studies.

The final section, Depositional History of the Kreftenheye Formation, presents a more detailed depositional history of the Kreftenheye Formation. It describes the depositional environments, geological timeframes, and specific characteristics of its members and beds. This geological context is essential for interpreting the data analysis results presented later in the thesis.

By integrating these three elements, the literature review aims to build a solid foundation for the subsequent database analysis. This will facilitate a deeper understanding of the Kreftenheye Sand Formation, enhancing the interpretation of results and the integration of geological and geotechnical knowledge.

2.1 Sand Overview

2.1.1 Geotechnical Relevance

In the heavily populated coastal and river areas of the Netherlands, the Kreftenheye Formation is typically overlain by clay and peat of Holocene age (Ngan-Tillard et al. (2010); Koster et al.

(2018)). Consequently, most infrastructure and buildings are founded on piles. These foundation piles are driven through the overlying soft sediment, transferring most of the load to the stiff sands of the Kreftenheye Formation. Research related to foundation piles and the Kreftenheye Formation is therefore very relevant, and some issues are highlighted below. Another example that highlights the relevance of this work is related to the current project "Meanderende Maas "(Meanderende Maas (2024); Boskalis (2024)). The geotechnical problems described below show the value of research in which field data is combined with geotechnical and geological knowledge.

Pile Installation in Dense Sand
As Duffy et al. (2024) and de Gijt et al. (2019) have shown in their work, installing a pile in dense sand can be challenging. Achieving the target depth often requires a very large force. However, it is crucial that the pile remains intact, as any defects can lead to failure. Therefore, installing piles in dense sand involves a careful balance between applying sufficient force and maintaining the structural integrity of the pile. It is important to know the exact ground conditions to anticipate the force needed to reach the target depth and to design a pile that is suitable for those conditions. Understanding more about the geotechnical measurements in the Kreftenheye Formation can be of great importance for this purpose.

Pile Capacity in Intermediate Weak Layers
Weak zones within a soil profile can greatly influence the bearing capacity of a foundation pile (Chai & Tehrani (2022); Duffy et al. (2024)). Interlayered floodplain or soft channel lag sediments sometimes occur within a sand formation, and it is crucial to identify and accurately model these layers to fully understand the response of the pile. From a geotechnical perspective, there is sometimes a lack of understanding regarding the extent of these layers and their variability, which highlights the relevance of this thesis.

Sheet Pile Walls Installation in Dense Sand
Sheet pile walls are water and soil retaining structures used to reinforce features such as dikes. In the "Meanderende Maas" project, the dense sand from the Kreftenheye poses significant challenges during the installation of the sheet pile walls. More than 17 kilometers of sheet piles needed to be installed to the correct depth and interlocked. In projects like this, anticipating ground conditions and understanding the variability of the soil can be crucial to success.

2.1.2 Sand characteristics

Sand is a type of soil composed of granular material, including weathered rock, biogenic material, and minerals. As a granular soil, its characteristics can be analyzed both at the grain level and in terms of its bulk properties. These measurements are essential for accurately describing and understanding the soil.

Grain characteristics

Grain size
The identification of coarse soils is based on the grain sizes, for finer material other identification methods are used. Table 2.1 shows an overview of the soil groups and their corresponding

grain size. A material is characterised as sand when the grain sizes are between 0.0063 mm and 2.0 mm according to Netherlands Standardization Institute (2020). It is important to recognize that soils often contain a range of grain sizes, which together define the grain size distribution, as discussed in the section on bulk properties.

Table 2.1: Grain sizes from NEN 14688-1 (Netherlands Standardization Institute (2020))

		Particle size fractions	**Range of particle sizes** $[mm]$
Very coarse soil	Gravel (Gr)	Coarse Gravel (cGr)	$> 20 \leq 63$
		Medium gravel (mGr)	$> 6.3 \leq 20$
		Fine gravel (fGr)	$> 2.0 \leq 6.3$
Coarse soil		Coarse sand (cSa)	$> 0.63 \leq 2.0$
		Medium sand (mSa)	$> 0.20 \leq 0.63$
		Fine sand (fSa)	$> 0.063 \leq 0.20$
Fine soil	Silt (Si)		$> 0.002 \leq 0.063$
	Clay (Cl)		≤ 0.002

Grain shape

The shape of the grain can be described by the sphericity and roundness which is shown in Figure 2.1 from Krumbein (1941). The examination of grains involves the utilisation of microscopes, such as an optical, scanning electron, or other types, depending on the specific requirements of the study. However, this approach can be subjective as it relies on human judgment, making it less quantitative. Research by Cox & Budhu (2008) highlights that light microscopy, when focused on key shape parameters such as circularity, roundness, compactness, sphericity, aspect ratio, and modified ratio, enhances the robustness of the interpretation. Additionally, static image analysis software offers further advantages by providing a more consistent and quantative examination of grain shape.

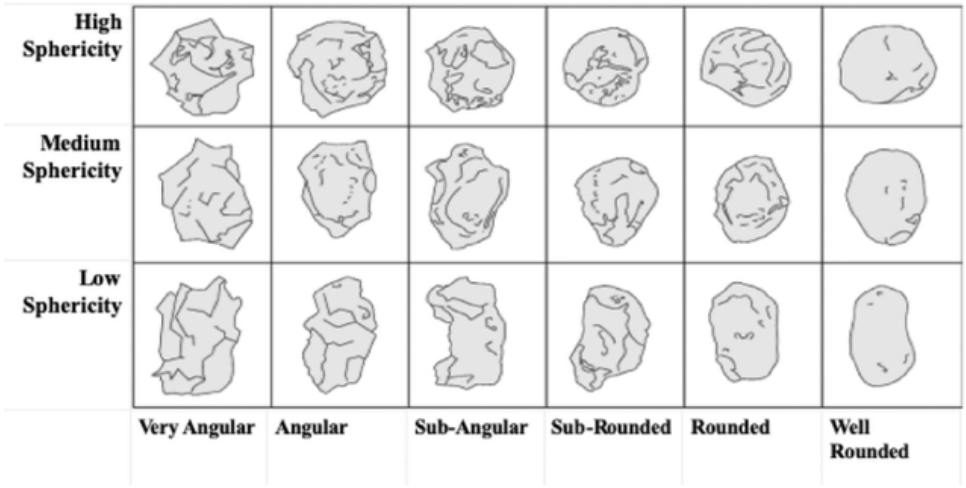

Figure 2.1: Classification by roundness and sphericity of grains, from Krumbein (1941), modified by Ulusoy (2019)

Mineralogy and other components

The sand grains can consist of different minerals, the most common ones being quartz, feldspar, and mica. The grains can also include fragments from preexisting rocks (lithic fragments), calcium carbonate shell fragments (biogenic particles), or crystalline structures that grow from minerals (authigenic minerals). These minerals and fragments have properties such as hardness and resistance to weathering, which influence the bulk properties of the sand. Therefore, it is important to identify the minerals and fragments that are present (Nichols (2009)).

Furthermore, the spaces between the grains can contain cementation, bonding, or filling materials. Cementation involves the precipitation of minerals between the grains, effectively gluing them together. This process often occurs in calcareous sands, which may be present in the dataset. Bonding introduces various types of connections among the grains, such as chemical bonds or mineral-to-mineral bonds. Lastly, the voids between grains can be filled with different materials, often in minor amounts.

Bulk characteristics

Grain size distribution

One of the key properties to describe a soil is the grain size distribution because it provides valuable information on the properties and behaviour of the soil. Most commonly, a sieve analysis is done to determine the grain size distribution and the result is plotted in a graph called the grain size distribution curve, an example is given in Figure 2.2. Sieve analysis can be done dry or wet, depending on the objectives of the study. Dry sieve analysis is typically used for cohesionless soils, such as sand and gravel. It is a more straightforward method, suitable for materials that do not clump together. Wet sieve analysis is used for cohesive materials, such as clayey soils. This method involves adding water to prevent clogging of the sieves and facilitate the separation of fine particles. This method is generally more time-consuming.

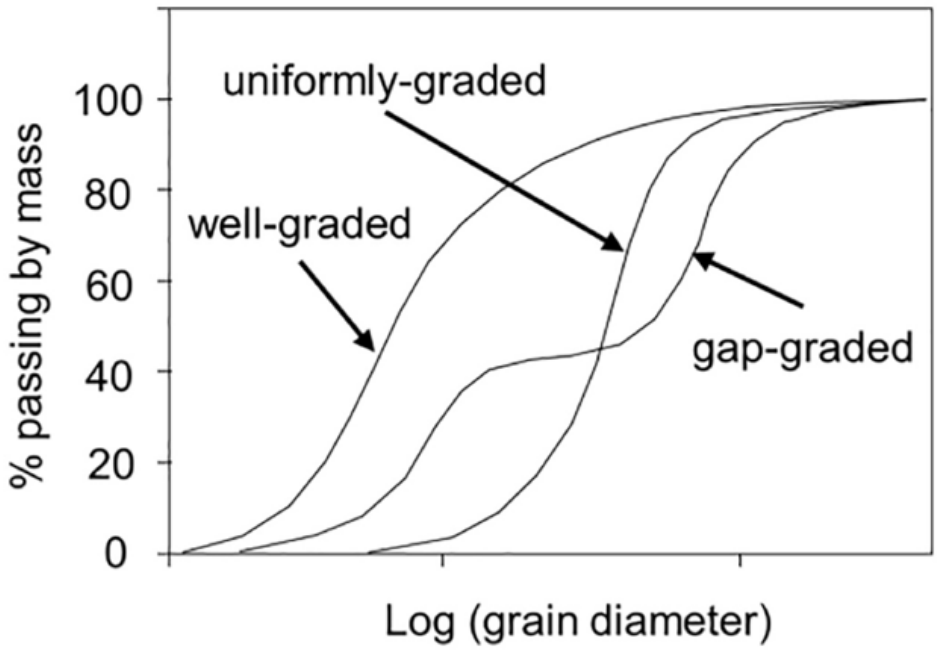

Figure 2.2: Schematic example of a grain size distribution plot from Zhang et al. (2018)

It should be noted that the sieves used in grain size distribution tests have square-shaped holes, while soil particles can have various shapes. Therefore, the test results may not perfectly represent the actual soil structure. The obtained grain size distribution can be described or quantified by certain terms and parameters, which are explained below (Lambe & Whitman (1991)).

- **Uniformly graded soil**: This soil consists of predominantly one particle size.
- **Well-graded soil**: This soil consists of a wide range of particle sizes.
- **Gap-graded soil**: This soil consists of a mix of small and large particles, but very few intermediate sizes.
- $\boldsymbol{D_{70}}$: The sieve size at which 70% of the soil particles pass through.
- **Uniformity coefficient ($\boldsymbol{C_u}$)**: A dimensionless measure of the degree of uniformity of the grain sizes, defined as:

$$C_u = \frac{D_{60}}{D_{10}} \quad [\text{-}] \quad (2.1)$$

- **Coefficient of curvature ($\boldsymbol{C_c}$**: A dimensionless measure of the curvature of the grain size distribution curve, defined as:

$$C_c = \frac{D_{30}^2}{D_{60} D_{10}} \quad [\text{-}] \quad (2.2)$$

- **Fines content (FC)**: Expresses the fines content ($\leq 0.063\,\mathrm{mm}$) as a percentage of the total weight of the soil:

$$FC = \frac{Weight\ fines}{Total\ Weight\ of\ Soil\ Sample} \times 100\% \quad [\%] \quad (2.3)$$

These parameters and terms help in characterizing and comparing different soil samples based on their particle size distribution.

In addition to sieve analysis, the particle size distribution can be determined using other advanced methods, such as image analysis and laser diffraction. The image analysis technique involves using a microscope to capture digital images of the grains, which are then processed to determine the grain size distribution. The laser diffraction technique, used in the dataset for this thesis, involves directing a laser beam at the soil sample and measuring the angles at which light is scattered. This scattering data allows for the determination of grain size. A more detailed description of the laser diffraction technique can be found in subsection 2.2.2. Both image analysis and laser diffraction offer improved measurement of grain shape parameters, addressing the limitations inherent in sieve tests.

Density

In soil mechanics, the density of a soil can be expressed in numerous ways, this section will go through the most used ones. The bulk density of a soil is the mass per unit soil volume and it is the most straightforward expression of the density.

$$\rho_b = \frac{M}{V} \qquad [\text{kg/m}^3\ ] \quad (2.4)$$

Where:

M = Mass [kg]
V = Volume [m^3]

The relative density of a soil, however, refers to the packing of the particles and resulting voids. It is calculated using the void ratio e and is expressed as a percentage. When RD is 0%, the soil is in the most loose state, when RD is 100%, the soil is fully compacted. In the equation e_{max} is the maximum void ratio of the soil, so the loosest state, and e_{min} is the minimum void ratio, so the densest state. e can be calculated using Equation 2.1.2 and RD with Equation 2.1.2.

$$e = \frac{V_v}{V_s} \qquad [\text{-}] \quad (2.5)$$

$$RD = \frac{e_{max} - e}{e_{max} - e_{min}} \times 100\% \qquad [\%] \quad (2.6)$$

Where:

V_v = Volume void space [m^3]
V_s = Volume solids [m^3]

Packing, porosity and void ratio
The arrangement of particles is called the packing of the soil. The packing affects different bulk properties, such as porosity and relative density for example. The packing of soil is dependent on the grain properties (e.g. particle size, sphericity and roundness). The packing can be expressed with the following variables, bulk density, porosity, void ratio and packing density. (Panayiotopoulos (1989))

2.1.3 Soil Deposition

To understand the characteristics of the Kreftenheye Formation, it is essential to examine the processes of soil deposition and their influence on soil properties. These processes can be described by the sedimentary soil cycle, illustrated in Figure 2.3, which includes weathering, transportation, deposition, and finally, burial.

The transportation and deposition phases of the sedimentary cycle are critical in shaping the depositional environment, which in turn influences the characteristics of the Kreftenheye Formation. Since the Kreftenheye Formation is a fluvial deposit, it is essential to focus on fluvial depositional environments in particular. Consequently, these steps are highlighted in the flowchart, and the fluvial depositional environments will be discussed in detail.

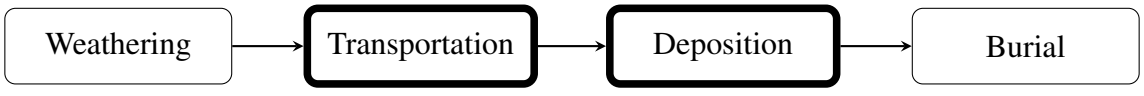

Figure 2.3: Sedimentary cycle of soils

Weathering

The sedimentary soil cycle begins with the weathering of the parent rock, a process that involves the breakdown and dissolution of the rock through chemical, mechanical, or biological processes.

- **Chemical Weathering:** Involves the alteration of the rock's mineral composition through reactions with water, air, and other chemicals.
- **Mechanical Weathering:** Breaks the rock into smaller fragments without altering its chemical composition, often through processes like freeze-thaw cycles, abrasion, and pressure release.
- **Biological Weathering:** Involves the actions of plants, animals, and microbes that can cause the rock to fracture, break down, or dissolve.

These processes and their results are detailed in the book by Pettijohn (1987), which provides a comprehensive overview of sedimentary processes and their implications for soil and rock formation.

Transportation

The next step in the sedimentary cycle is the transport of sediment. Various transporting agents significantly affect the erosion, size, shape, and surface characteristics of sediment, as well as its sorting properties. Table 2.2 provides an overview of the effects of transportation by water, air, ice, gravity, and organic processes.

One notable observation from the table is that transportation by wind (air) tends to result in a high degree of rounding of the grains. This is primarily due to the abrasive action of wind-blown particles on the surface of the sediment grains as they are transported over land. Over time, this constant abrasion smooths the edges and surfaces of the grains, leading to their rounded shape. For example, in the Dutch Boxtel Formation, sand grains transported by wind are often referred to as "sand marbles" due to their pronounced roundness. Unfortunately, the dataset used in this thesis does not include information on grain surface texture, so this aspect cannot be analyzed directly. However differences in CPT response between the Boxtel and Kreftenheye Formations could be attributed to the variations in transport agents and their effects on surface texture.

Additionally, transportation by water has a profound impact on the sorting of sediment compared to other transportation methods. This is because water can carry a wide range of sediment sizes and densities over long distances, allowing for extensive sorting by size and weight. The turbulent flow of water can selectively transport finer particles while leaving behind coarser grains, resulting in well-sorted sediment deposits. This influence on sorting will be further investigated in the dataset analysis, as it offers valuable insights into the depositional processes and sedimentary environments.

Table 2.2: Effects of transportation on sediments (Lambe & Whitman (1991))

	Water	Air	Ice	Gravity	Organic
Size	Reduction through solution	Considerable reduction	Considerable grinding and impact	Considerable impact	Minor abrasion effects from direct organic transportation
Shape and roundness	Rounding of sand and gravel	High degree of rounding	Angular, soled particles	Angular, non-spherical	-
Surface texture	Sand: smooth, polished, shiny Silt: little effect	Impact producer frosted surfaces	Striated surfaces	Striated surfaces	-
Sorting	Considerable sorting Marine: uniformly sorted River: well sorted	Impact producer frosted surfaces	Very little sorting	No sorting	Limited sorting

Fluvial Depositional Environments

A depositional environment is a setting where sediments accumulate over time, influenced by various factors such as climate, topography, and vegetation. These environments can be classified into several types, including glacial, fluvial, marine, and aeolian, each with its own subenvironments and distinct characteristics. Since the Kreftenheye Formation is a fluvially deposited formation, this section focuses specifically on fluvial depositional environments. Classification of these environments follows the framework proposed by TNO-GSN (2024). A detailed description of the different fluvial environments is provided below:

- **FFG (Fluvial, channel - high-energy)**: This depositional environment represents river channels characterized by high energy. This is often attributed to significant elevation changes between the source and sink over a relatively short distance, typically with sparse vegetation in the surrounding area. Braided river systems are the most common example of this depositional environment. In these systems, the rapid flow of water, frequent changes in discharge, and sediment load contribute to the deposition of coarser sediments such as coarse sand and gravel. Figure 2.4 illustrates an example of such a system.

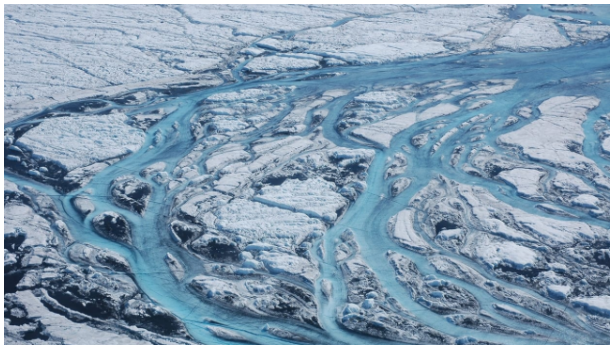

Figure 2.4: Example FFG, braided river (retrieved from: Science (2018))

- **FFZ (Fluvial, channel - slightly less energy)**: Similar to FFG, this environment represents areas within river channels, but with slightly lower energy levels. Sediments deposited here range from moderate fine to moderate coarse, indicating a somewhat less energentic hydraulic regime compared to FFG. Figure 2.5 illustrates an example of such a system.

Figure 2.5: Example FFZ, meandering river (retrieved from: Ecopedia (2024))

- **FFKLA (Fluvial, lake and residual channel)**: This environment comprises sediments deposited in lakes and residual channels within a fluvial system. These areas are no longer part of the active river system, leading to the deposition of finer sediments such as clay and peat due to stagnant or slow water flow. Figure 2.6 shows an example of a residual channel.

Figure 2.6: Example FFKLA, residual channel (retrieved from: Natuurkennis (2024))

- **FFKMA (Fluvial, overbank)**: This depositional environment signifies regions of low energy within river systems, such as floodplains, where sedimentation of clay soils occurs due to the presence of still water. Figure 2.7 shows an example of a floodplain.

Figure 2.7: Example FFKMA, floodplain (retrieved from: EOS (2023))

- **FFL (Fluvial, bank and crevasse)**: This environment encompasses the banks of rivers and areas where crevasses or breaches occur. Sediments deposited here are influenced by both fluvial processes along the riverbanks and by the formation of crevasses, which may result from changes in water flow. Figure 2.8 shows an example of a riverbank.

Figure 2.8: Example FFL, River bank (retrieved from: Gebiedsontwikkeling.nu (2023))

- **FOVAM/FOVEU (Marsh-like)**: The final depositional environment in the dataset represents marshland. These areas can remain wet for extended periods, leading to the deposition of fine-grained, organic-rich sediments enriched with accumulated plant material. Figure 2.9 provides an example of what this depositional environment looks like.

Figure 2.9: Example FOVAM/FOVEU, marsh land (retrieved from: Geographic (2024))

Burial
The burial stage in the sedimentary cycle involves the progressive covering of sediments by additional layers, driven by the creation of accommodation space through tectonic subsidence and eustatic sea-level changes. Tectonic activity, such as plate movements, significantly influences the formation of sedimentary basins and the rate of sediment accumulation.

2.1.4 Dutch Lithostratigraphic Units

Lithostratigraphy is the ordering of the layers in the Earth based on the characteristics of the soil and rock layers. In this classifciation system, the hierarchy includes Groups, Formations, Members, and Beds.

This thesis focusses on the Kreftenheye Formation, which is part of the Boven-Noordzee Group. Most of the soil within the Kreftenheye Formation is only part of the formation. However there are distinct members in the formation such as the Ockenburg, Zutphen, Twello, en Well Members. Lastly, there is one bed called the Wijchen Bed.

To provide context about the subsurface formations in the Netherlands, a brief overview of several formations is presented. In the western part of the country, the Eem Formation in North Holland and the Urk Formation in South Holland are typically found beneath the Kreftenheye Formation. In the eastern regions, the Kreftenheye Formation is underlain by the Waalre Formation. Moreover, large areas of the Kreftenheye Formation across the Netherlands are overlain by the Boxtel Formation.

Eem Formation
The Eem Formation was deposited during the Upper Pleistocene, a period marked by rising sea levels that caused the sea to advance into glacial basins. This led to the accumulation of marine deposits consisting of fine sand and clay. The formation typically has a thickness of about 15 meters, but it can reach up to 70 meters in some glacial basins (TNO-GSN (2024)).

Urk Formation
The deposition of fluvial and estuarine sediments from the Urk Formation occurred during the late Cromerian to middle Saalian periods. This formation varies in thickness from about 30 to 60 meters and comprises fine to coarse sand, occasionally interspersed with thick clay layers. At the top of this formation, the Kreftenheye is found, where the sand transitions to gravel and river sand (TNO-GSN (2024)).

Waalre Formation
The Waalre Formation consists of fluvial and estuarine deposits from the Rhine, and it contains a variety of depositional environments. It was deposited during the late Pliocene to early Pleistocene and can attain thicknesses of up to 140 meters. The boundary between the Kreftenheye Formation and the Waalre Formation is characterized by a transition from the coarser gravel and river sand of the Kreftenheye to the different sediment composition of the Waalre (TNO-GSN (2024)).

Boxtel formation
The Boxtel formation was deposited during the upper Pleistocene and Holocene when the

Northern part of the Netherlands was covered by ice sheets and the southern part was a periglacial area. Under these periglacial conditions in the south, aeolian sands (dekzanden and löss) and local river dunes were deposited. The formation is about 10 to 35 metres thick, and comprises mostly of aeolian sediments that contain very rounded grains (TNO-GSN (2024)).

2.2 Background on Testing Methods

2.2.1 Cone Penetration Test

The cone penetration test (CPT) is the most widely used method for characterising the subsurface in the Netherlands. It is a fast and relatively inexpensive technique, particularly very suitable for the Dutch medium to soft soils. Consequently, there exists a substantial database available of cone penetration measurements of the Dutch subsoil. To effectively study these databases, it is important to comprehend the basics of the test, the procedures for correcting the measurements, and the methodologies for interpreting the test, and earlier research on CPT interpretation of geological deposits.

During the cone penetration test a steel rod with a cone-shaped tip is pushed into the soil that measures the resistance. Load cells are measuring the resistance at the tip of the cone (tip resistance) and around the sleeve (sleeve resistance). Additional sensors, such as temperature, pressure, or electrical resistivity sensors (with the most common being the pore pressure sensor), can be added to the device. Figure 2.10 provides an overview of the geometry of the cone.

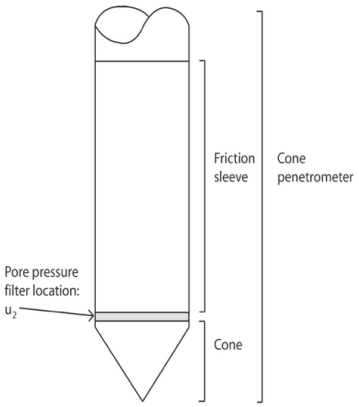

Figure 2.10: Geometry of the cone penetrometer from Robertson & Cabal (2014)

The Dutch standard NEN22476-1 (Netherlands Standardization Institute (2012)) prescribes the standard test procedures. Key requirements include the penetration rate falling within a specified range of 20 ± 5 mm/s, the penetration trajectory having a maximum deviation of 2° from the ground surface and the measurements being taken at regular intervals of 20 mm. Four accuracy classes (0, 1, 2, and 3) are defined, with lower numbers indicating a higher level of required accuracy. Regular calibration of the sensors against reference load cells and transducers is necessary for reliable testing results.

Corrections
Before analysing cone resistance and sleeve friction measurements, a correction related to the pore water pressure should be applied in soft clays and silts according to Campanella et al. (1982) , in sandy soils this is not necessary.

$$q_t = q_c + u_2(1 - a) \quad \text{[MPa]} \quad (2.7)$$

Where:

q_t = Corrected cone resistance [MPa]
a = Net area ratio [-]
u_2 = Water pressure at top of sleeve [MPa]

$$f_t = f_s - (u_2 A_{sb} - u_3 A_{st})/A_s \quad \text{[MPa]} \quad (2.8)$$

f_t = Corrected sleeve friction [MPa]
A_{sb} = Cross-sectional area of the bottom of the friction sleeve [mm^2]
u_3 = Pore pressure 3 [MPa]
A_{st} = Cross-sectional area of the top of the friction sleeve [mm^2]
A_s = Cross-sectional area of the bottom of the friction sleeve [mm^2]

The corrected cone resistance and sleeve friction can also be normalised by the vertical stress, so data from different depths can be compared (Robertson & Cabal (2014)).

$$Q_t = (q_t - \sigma_{v0})/\sigma'_{v0} \quad \text{[-]} \quad (2.9)$$

Where:

Q_t = Normalised cone resistance [-]
σ_{v0} = Total vertical stress [MPa]
σ'_{v0} = Effective vertical stress [MPa]

$$F_r = (f_s/(q_t - \sigma_{v0})) \times 100\% \quad \text{[\%]} \quad (2.10)$$

Where:

F_r = Normalised friction ratio [$\%$]

Additionally, one must be careful, as other factors like temperature and wear can cause deFormations in the cone shape, leading to inaccurate measurements in the strain gauges. Soil layering can also influence measurements due to the detection distance of the CPT (Lunne T. (1997)).

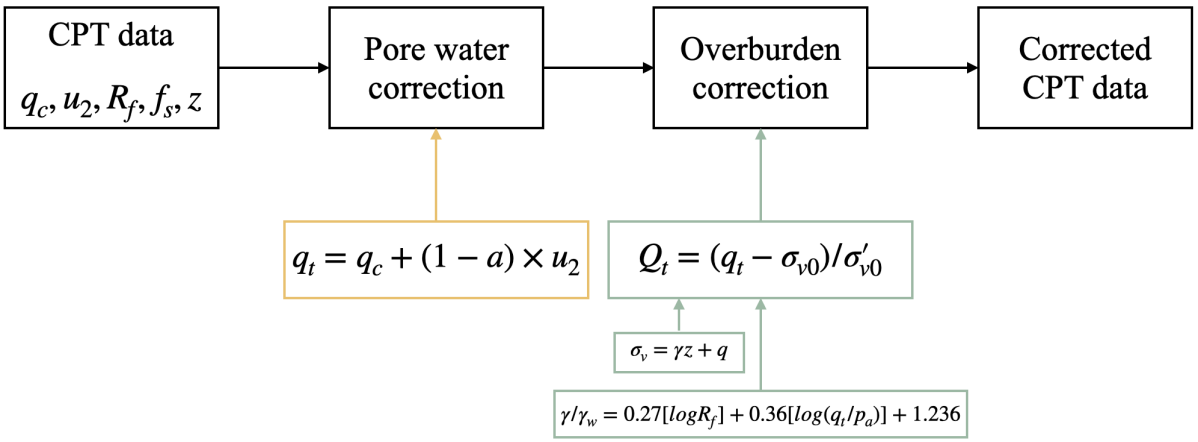

Figure 2.11: Schematic overview of standard CPT corrections

CPT Interpretation

- **Texture-based classification system**
  Robertson (1990) proposed a chart based on the normalised friction ratio and the normalised cone penetration resistance to identify soil texture types. The classification system is in good agreement for soils with little microstructure or texture. The chart is shown in 2.12 and uses the following equation from Robertson (1990). This classification system is used in this thesis because of its common use and enhances scientific reproducibility.

$$I_C = [(3.47 - logQ_t)^2 + (logF_r + 1.22)^2]^{0.5} \quad [\%] \quad (2.11)$$

  Where:

  $I_C =$ Soil Behaviour type index [%]

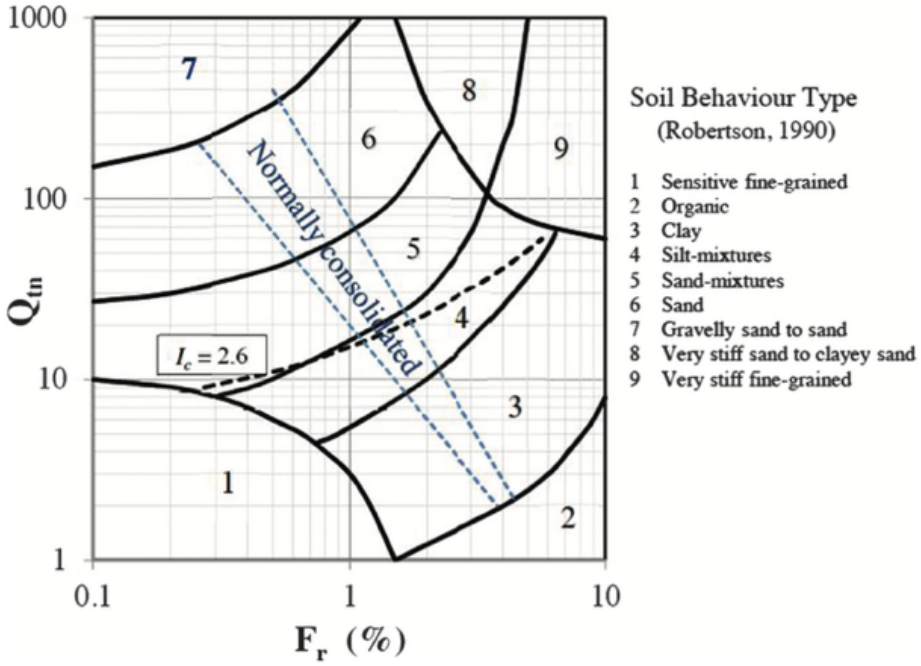

Figure 2.12: Texture-based classification system from Robertson (1990)

- **Schneider chart**
  Schneider et al. (2008) observed that Robertson (1990) texture-based classification system did not work well with North Sea data, prompting him to propose a new chart based on piezocone parameters, specifically pore water pressure and normalised cone resistance. This new chart is particularly useful for offshore applications.

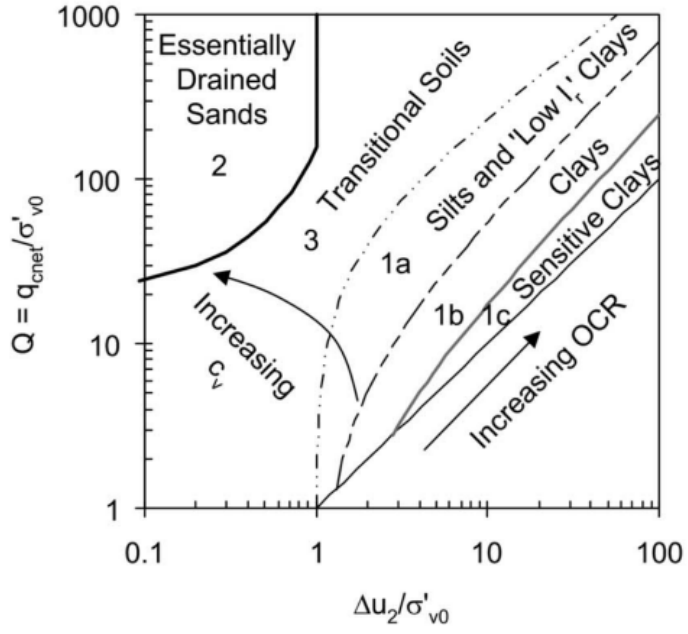

Figure 2.13: Piezocone soil classification chart from Schneider et al. (2008)

- **Behaviour type chart**
  In 2016, Robertson proposed an updated version of the charts from Robertson (1990), Robertson (2009), and Schneider et al. (2008). These updates classify soils based on their behavior rather than texture. Behavior classification provides a more direct correlation with laboratory data compared to texture classification. Additionally, behavior classification offers more relevant information for geotechnical applications.

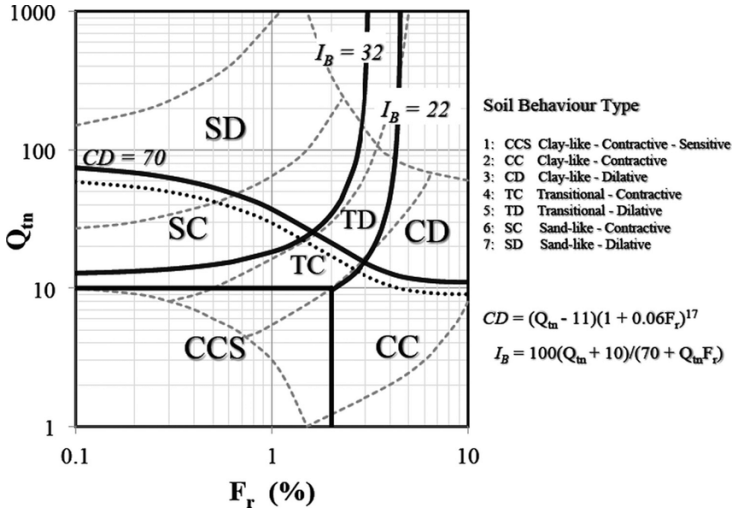

Figure 2.14: Behaviour based classification from Robertson (2016)

- **Dutch soil charts**
  Lastly, a soil chart adapted from Robertson (1990) was specifically tailored by FUGRO Ingenieursbureau B.V. (2010) to fit Dutch soils. This chart includes consolidated peat as an additional soil type and indicates the most common subsurface formations.

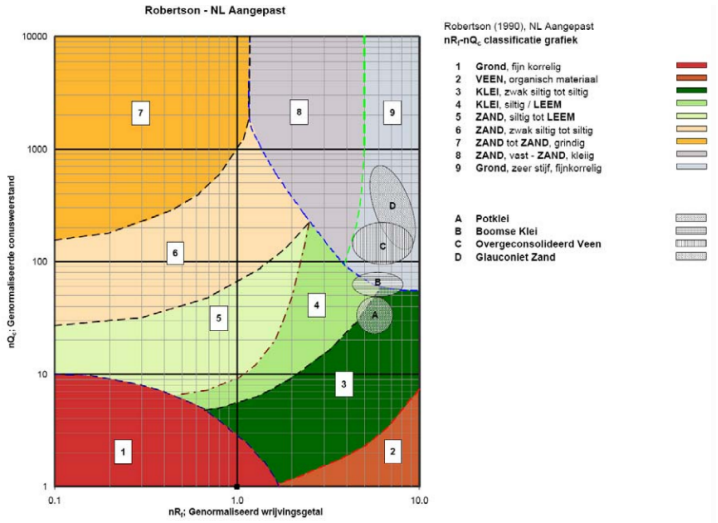

Figure 2.15: Dutch Soil classification chart adapted from Robertson (1990) by FUGRO Ingenieursbureau B.V. (2010)

Limitations and uncertainties
CPT measurements are subject to a number of limitations and uncertainties that can influence the results, as discussed by Lunne T. (1997). Some of the most important ones are outlined below:

- **Effect of Wear and Temperature**: Wear on the cone tip can lead to variations in the cross-sectional area, which can significantly affect the accuracy of the measurements. Temperature variations can also affect the readings because of their influence on the strain gauges. This underscores the importance of calibration of the cone.
- **Sensing Distance**: The cone resistance is influenced by the material both ahead of and behind the cone tip. This can result in inaccurate measurements of the mechanical properties of the soil, especially in thin-layered deposits where extra care must be taken to interpret the data correctly.
- **Overburden Stress**: The measurements obtained from CPT are influenced by overburden stress, with cone resistance typically increasing with depth. Early classification charts were based on penetration depths of up to 30 meters. For CPT data obtained at greater depths, extra caution must be exercised in the interpretation to account for the effects of overburden stress.

Previous studies on CPT characterisation of deposits
Amorosi & Marchi (1999) plotted facies associations on a Robertson chart, demonstrating excellent correlations between CPT zones and facies at a local scale. However, these correlations are not applicable on a global scale. While their study integrates geological and geotechnical data with a focus on facies at a local level, this thesis will concentrate on formations and members in the Dutch subsurface.

Lafuerza et al. (2005) used CPT and CPTu data to characterize deltaic sediment facies and construct a 3D model. Their work demonstrated that a highly detailed model can be created using local CPT data, allowing for the distinction of different sediment bodies. Despite this, borehole data remains essential. While this study is focused on a local scale and specific sediment bodies, it highlights the potential of CPT data for detailed subsurface characterization.

Schiltz (2020) utilized 200 CPTs within an area of 60 km², enabling a very detailed local analysis of the subsurface. Schiltz demonstrated that CPT data can be effectively used to identify stratigraphic boundaries and make sedimentological interpretations. In contrast, this thesis addresses a much larger area, which makes interpretation more challenging due to larger variations in the data.

Schokker & Koster (2004) studied the sedimentology and facies of the Boxtel formation during the Pleistocene using sedimentary cores, cone penetration tests, and grain size data in the area of Noord-Brabant in the Netherlands. They effectively linked the CPT and grain size data to the depositional history of the area. This thesis aims to conduct a similar study but on a larger scale, focusing on the geotechnically relevant Kreftenheye Formation.

2.2.2 Particle Size Analysis

Laser diffraction (LD) is a technique used to determine particle size distribution by measuring the forward diffraction of a laser beam as it passes through a sample (Eshel et al. (2004)). The angle of diffraction is used to estimate particle size, while the intensity of the diffraction pattern provides information about the number of particles. Two primary optical models are employed to calculate the grain size distribution: the Fraunhofer diffraction model and Mie theory.

One of the key advantages of laser diffraction is its efficiency and accuracy. Analysis can be completed in a short time frame, typically 5-10 minutes per sample, and the method is highly repeatable across a wide range of particle sizes and fractions.

The workflow for laser diffraction analysis, as described by Treviranus (2013), involves several critical steps:

Sample Preparation: Ensure that particles are well-dispersed and suspended in the medium.

- System Preparation: Reduce existing noise in the system and perform blank alignment to ensure accurate measurements.
- Sample Analysis: Introduce the sample at the appropriate concentration and pump it through the system.
- Data Retrieval and Processing: Obtain the diffraction data and apply optical models to derive the grain size distribution.

Uncertainties in this method primarily stem from sample preparation. Proper sample dispersion and preparation are crucial for obtaining reliable measurements

2.3 Depositional History of the Kreftenheye Formation

2.3.1 Geological Time Frame

The Kreftenheye Formation was deposited by the river systems Rhine and Meuse in the Netherlands, commencing during the late Middle and Late Pleistocene, spanning approximately 160,000 to 12,000 years ago (Busschers (2008); Peeters et al. (2015); Verbraeck (1983); Busschers et al. (2005)). This timeframe encompasses the late Saalian (cold climate, glaciation), Eemian (warm climate), Weichselian (cold and temperate climate), and Holocene (warm climate) periods, each characterized by distinct climate conditions and sea levels as shown in Figure 2.16. The diverse climatic and environmental conditions over this extensive timescale resulted in fluvial deposits that include a wide range of sediment facies. Consequently, most of the Kreftenheye Formation is characterized by fine to coarse-grained sands and gravel, interspersed with thin layers of clay and peat (TNO-GSN (2024)).

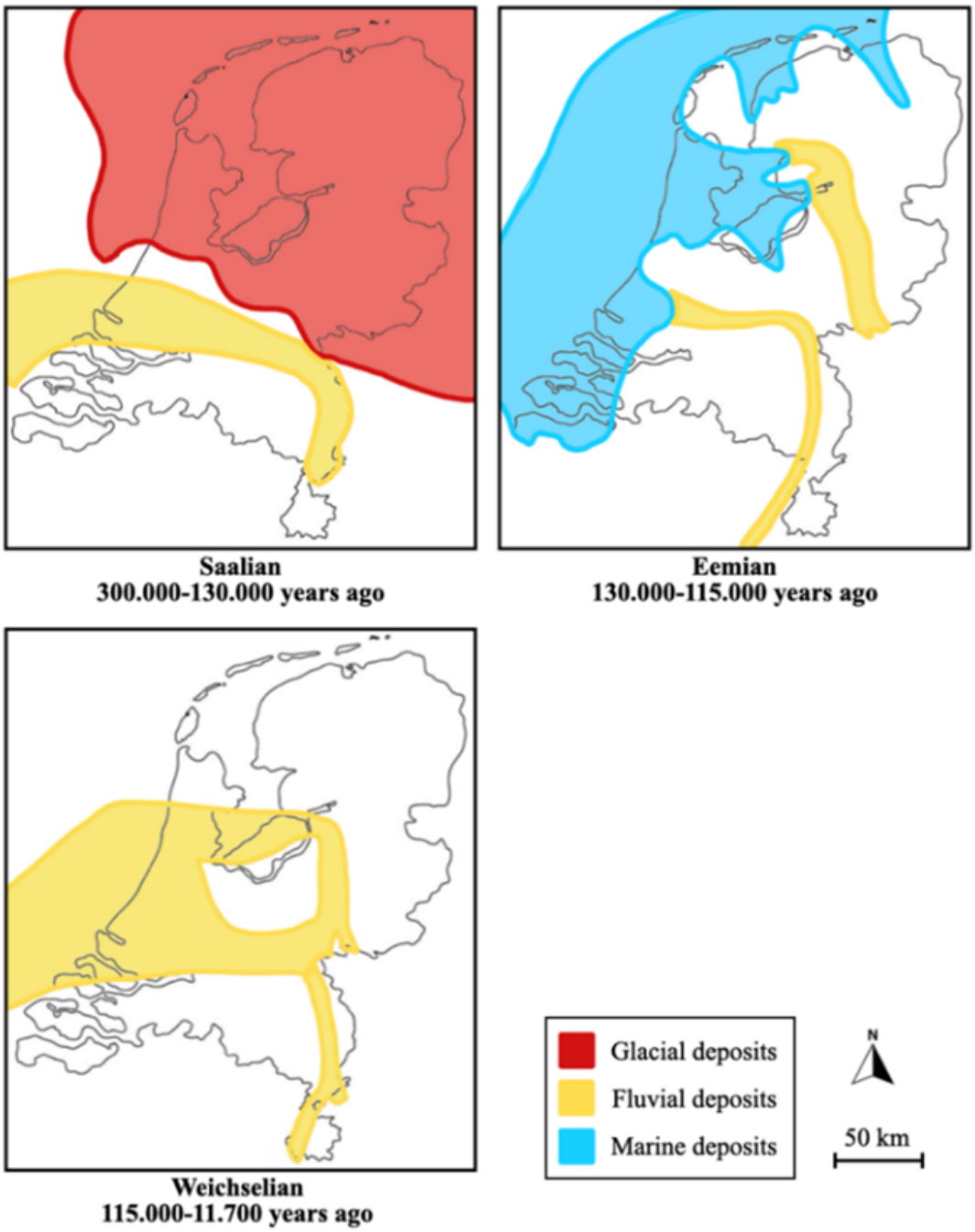

Figure 2.16: Simplified paleogeographical maps of the Netherlands during the late Saalian, Eemian, and Weichselian periods. Adapted from Busschers et al. (2007) and Wong et al. (2007)

Saalian - Glacial period

During the late Saalian glaciation, which occurred approximately 160.000 to 130.000 years ago, the northern region of the Netherlands experienced extensive glaciation with the ice sheet prograding into the Netherlands up-to the Haarlem – Utrecht – Nijmegen – Dusseldorf line (Figure 2.16). This glaciation led to the formation of ice-pushed ridges along the ice front, where fluvial sediments from the Rhine-Meuse system were deposited, contributing to the older part of the Kreftenheye Formation. As the late Saalian deglaciation unfolded, the Rhine shifted

its course into the former glaciated area, while the Meuse remained situated south of the former ice line (Peeters et al. (2015)).

The cold climate during this period resulted in a notably low sea level, creating significant height differences in the river system and fostering the development of highly energetic braided river systems. These rivers, which aligned with the contours of the ice sheet, facilitated the transport of meltwater and coarse-grained sediments, including glacial till (Busschers (2008)). Additionally, the persistently cold conditions led to a tundra landscape with scarce vegetation and permafrost, which contributed to the formation of eolian deposits (e.g. Boxtel Formation). Sedimentological records from the late Saalian reveal the presence of green, red, and black sandstones and shale fragments, which originated from the Eifel and Rhenish Massifs in Germany (Busschers et al. (2005)).

Eemian - Interglacial period
During the Eemian (130.000 to 115.000 years ago), the climate warmed, tree vegetation developed and sea-level rose to elevations similar to or above present day values, hereby submerging major part of the Netherlands. The encroaching coastline reduced the energy of the river systems, with dominance of deposition in meandering rivers, estuaries and shallow marine environments (Peeters et al. (2015)), this is shown in Figure 2.16. The river's course was shaped by the glacial basins that formed during the Saalian period (Busschers et al. (2005)).

Weichselian - Glacial period
In the subsequent Weichselian period (115.000 to 11.700 years ago), the Netherlands experienced a return to generally colder conditions with a strong drop in sea-level, formation of (temporal) permafrost and opening of the vegetation cover. Colder periods alternated with warmer climatic periods although especially the last 20.000 years of the Weichselian experienced most cold climatic conditions with large scale development of permafrost and supply of coarse-grained sediments into the high-energy Rhine-Meuse system, hereby depositing the upper part of the Kreftenheye Formation. During the second half of the Weichselian, the branch of the Rhine through the northern Netherlands became entirely abandoned and the Rhine retook a course south of the former late Saalian ice line, merging with the Meuse. The Sandstone in the sedimentary record highlighted the Rhenish Shield as a major source of sediments in this period. Additionally, reworked marine fossils from the Eemian period consistently contribute to the sediment composition in the western part of the Netherlands (Busschers (2008); Verbraeck (1983)).

2.3.2 Members

Most of the Kreftenheye Formation consists of fine to coarse-grained sand and gravel. However, it also includes five distinct Members and Beds: the Wijchen Bed, Ockenburg Member, Zutphen Member, Twello Member, and Well Member (TNO-GSN (2024)). The dataset in this thesis only contains Wijchen, Ockenburg, and Zutphen, therefore those will be discussed in more detail below.

Zutphen
The Zutphen member of the Kreftenheye Formation was deposited during the Eemian inter-

glacial period by a slow meandering Rhine. The river followed the contours of a former glacial basin from the Saalian period, as described by Peeters et al. (2020). At the convergence point between the sea and the Rhine, lacustrine and estuarine deposits consisting of clay and peat were identified, as reported in continuous cores by the research conducted by Busschers (2008).

Characteristic sediments in a meandering river system include fine-grained silts and clay deposits in the middle of the river, with sand accumulating along the riverbanks. Consequently, it is anticipated that the Zutphen member exhibits a variety of grain sizes and variable Cone Penetration Test (CPT) responses.

Borehole B15F1501 (Rutten) in Figure 2.17 , situated near the convergence point between the sea and the Rhine, shows the characteristic appearance of the fine-grained clay and peat deposits of the Zutphen member (indicated by the red lines). This contrasts with the coarser Kreftenheye sand found beneath the Zutphen member.

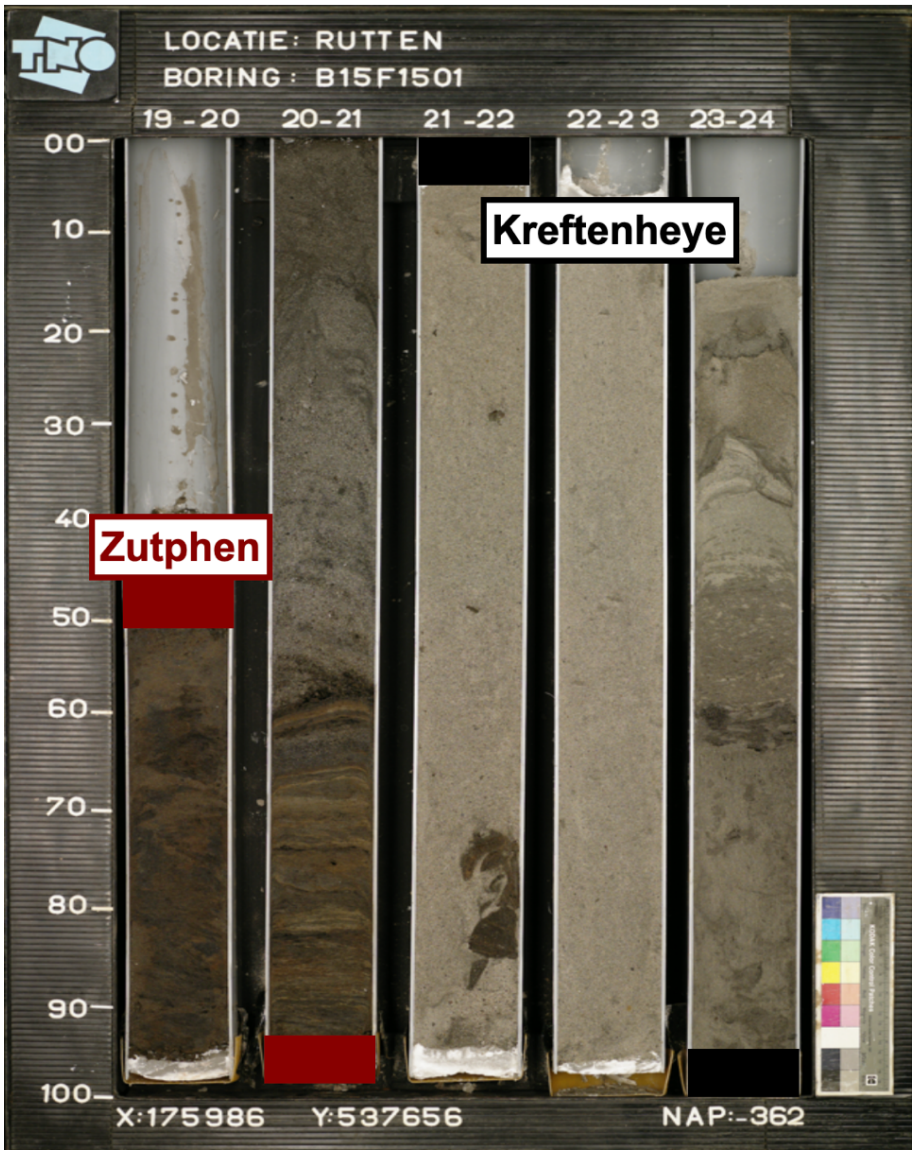

Figure 2.17: Borehole B15F1501 in Rutten retrieved from TNO-GSN (2024)

Ockenburg

The Ockenburg member of the Kreftenheye Formation was deposited during the Weichselian, the last glacial period, by a highly energetic braided river system. These river systems are characterized by a high volume of coarse sediment load and frequent migrations of river bars, resulting in fining upward sequences in their deposits. The elevated sediment load also induces greater erosion of previously deposited sediments. In this instance, the former sediments comprise marine shells from the Eemian period, when sea level was higher. This characteristic, identified as reworked marine fossils, distinguishes the Ockenburg member, as described by Busschers (2008). The Ockenburg member is predominantly found in Zuid-Holland and Zeeland, where the land was submerged during the Eemian period.

Borehole B30G4694 (Wassenaar), depicted in Figure 2.18, situated near the sea in Zuid-Holland, shows the characteristic reworked marine fossils from the Ockenburg member. Another notable feature observed in the borehole is the presence of channel lag, indicated by the rectangular boxes in the figure. Channel lag refers to the coarse sediment that accumulates at the bottom of a river channel. In some instances, clay particles can clump together to form clay nodules, which may also be included in the channel lag. Channel lag is a significant feature in boreholes as it provides insights into the rivers flow patterns. In areas with substantial channel lag, cone resistance measurements may be higher, leading to significant deviations in the measurement profile.

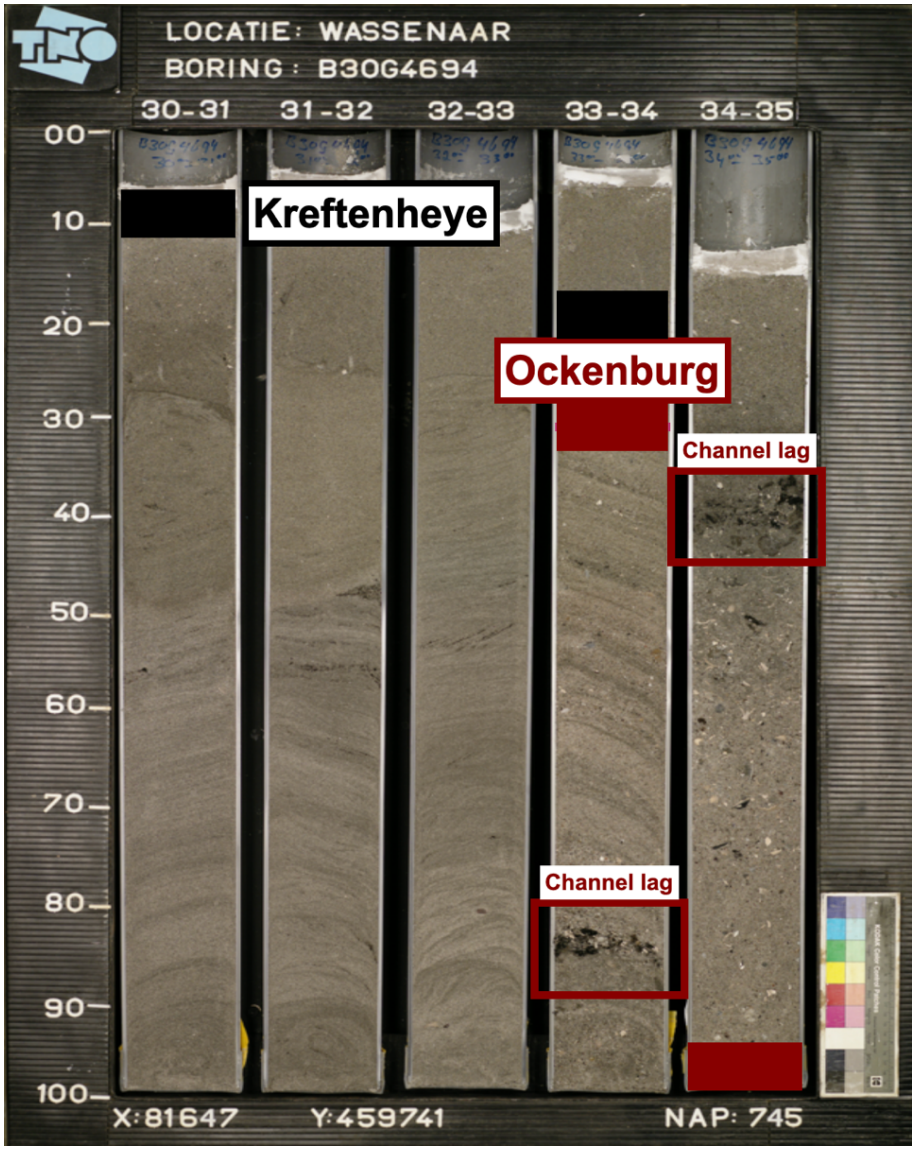

Figure 2.18: Borehole B30G4694 in Wassenaar retrieved from TNO-GSN (2024))

Wijchen

The Wijchen Member of the Kreftenheye Formation was deposited during the late Weichselian and early Holocene, marking a transition from the glacial to the current climate. During this period, rising sea levels and calmer river conditions led to the transformation of river systems into slow meandering channels.

These meandering rivers deposited clay sediments, along with some wind-blown fine-grained sands near their banks, which collectively characterize the Wijchen member Berendsen & Stouthamer (2000).

Borehole B37B3833 (s'Gravenzande), shown in Figure 2.19 and located in the western Netherlands, provides insight into the depositional characteristics of the Wijchen member. From depths of 22-23 meters, the borehole exhibits characteristics typical of floodplains near the Rhine, with the presence of very stiff clay sediments. The clay became stiff due to the drying of floodplain deposits over time, forming very stiff high OCR clays. The Wijchen members

seems to extend to depths of 21-22 meters, however this is not the case according to the borehole interpretation from TNO-GSN (2024). A similar type of clay is observed, but with a low OCR, indicating the presence of a flood basin rather than a floodplain. In a flood basin, water accumulates and deposits low OCR clays, which are not part of the Wijchen member.

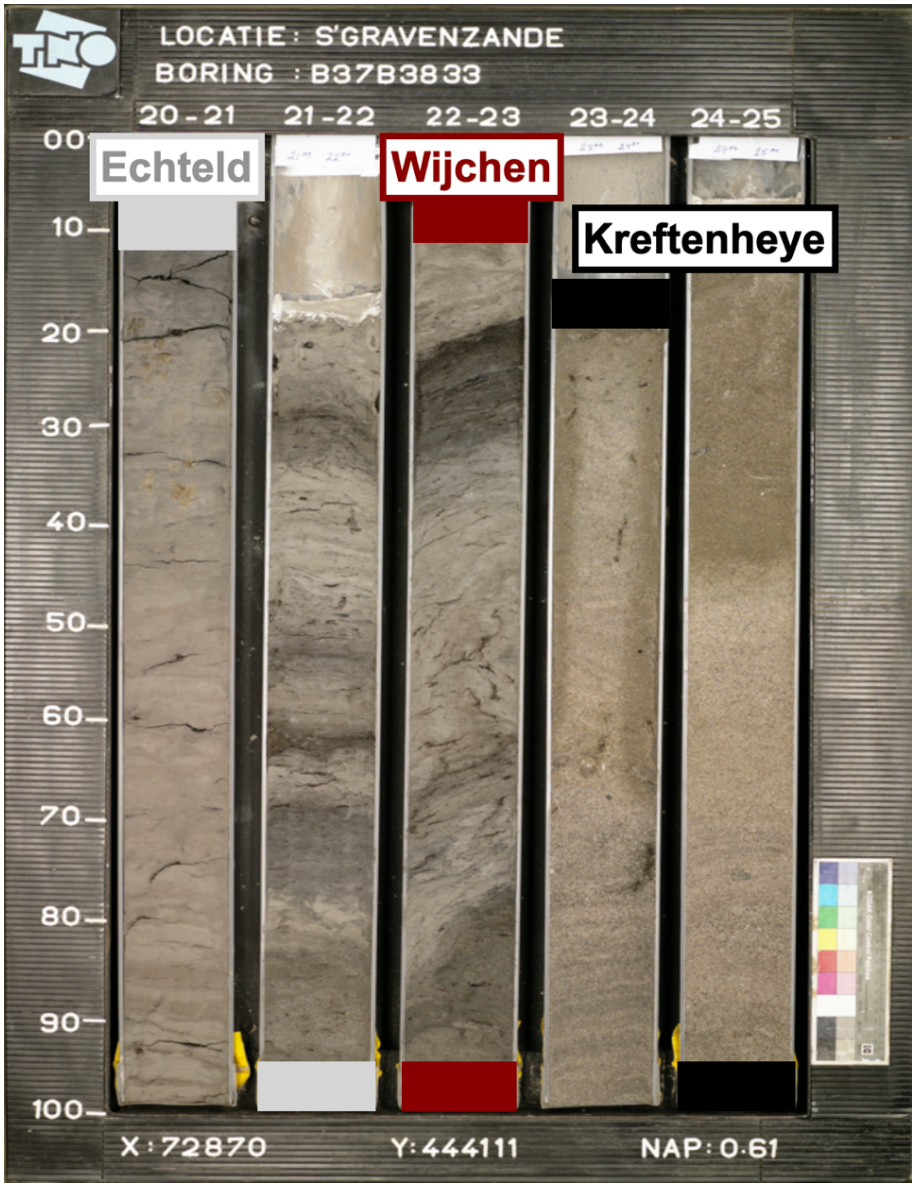

Figure 2.19: Borehole B37B3833 in s'Gravenzande retrieved from TNO-GSN (2024)

Area A and B

Busschers (2008) distinguished two areas within the undifferentiated Kreftenheye Formation based on the region and age: Area A, the upper/northern branch of the river system, deposited during the Weichselian and Eemian periods, and Area B, the lower/southern branch of the river system, deposited during the Saalian and Weichselian glacial period. Busschers (2008) described the differences between these areas based on continuous core samples; however, a detailed analysis based on CPT measurements has not yet been conducted. Figure 2.20 shows the

two areas on a map of the Netherlands.

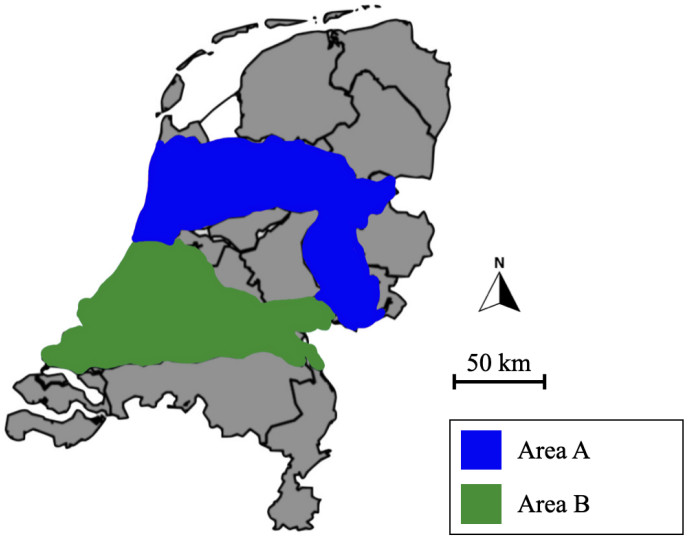

Figure 2.20: Area A and B Kreftenheye Formation

Chapter 3

Methods

This chapter outlines the methods used to achieve the goals of the research. The first section details the database, including a description, visualization, and validation of the dataset. The second section focuses on the Boulanger & Idriss (2014) CPT filter method, discussing its purpose, application, sensitivity, and examples.

3.1 Database

3.1.1 General Description

General aim

The dataset used in this thesis is from TNO - Geological Survey of the Netherlands and is collected as part of the drilling and measurement program TopIntegraal (e.g. Buma et al. (2024); Harting et al. (2023); Bosch et al. (2014); Vernes et al. (2010)). The dataset serves as a resource for characterizing subsurface conditions up to a depth of 30–50 meters in the Netherlands.

The objective of the TopIntegraal program is to provide detailed insights into subsurface characteristics to support for instance geological mapping, hydraulic assessments, and infrastructure planning. This is achieved through the integration of lithological, geochemical, geotechnical, and hydraulic data obtained from borehole trajectories and CPTs in the Netherlands. The dataset targets all the lithostratigraphic units defined in the shallow subsurface of the Netherlands and is running since 2006.

Source

Figure 3.1 shows an overview of the data locations in the Netherlands and the area of deposition of the Kreftenheye Formation. Each data point comprises two main components: a CPT sounding and a borehole. The CPT includes measurements of cone resistance, sleeve friction, and excess pore water pressure. The boreholes are sampled at different frequencies and intervals to capture the formation and its members. Data points are limited in the central eastern region of the Netherlands, as not all areas have been targeted yet in the ongoing TopIntegraal program. The acquisition and - in time - release of this data by TNO is expected in the future. The distance between the CPT and the borehole is intended to be limited as the CPT is performed first as an exploratory CPT before the drilling is performed. Three-quarters of the data points have the two main components lying within a 10-meter distance of each other.

The bar chart in Figure 3.2 displays the number of data points (CPT and borehole pairs) for the Kreftenheye Formation, indicating the number datapoints for the members. Additionally, the chart highlights in green the number of grain size measurements available within the formation and its individual members. CPT data for the formation and its members were selected based on the lithostratigraphic interpretations of the associated boreholes by TNO.

Figure 3.3 shows the specific locations of the Members, with the approximate deposition regions marked in pink. The Zutphen member contains 6 pairs and is sampled only locally. The Ockenburg member includes 18 data points and spans a large part of its depositional area. The Wijchen Member has 14 data points, primarily located in the central-west region of the Netherlands.

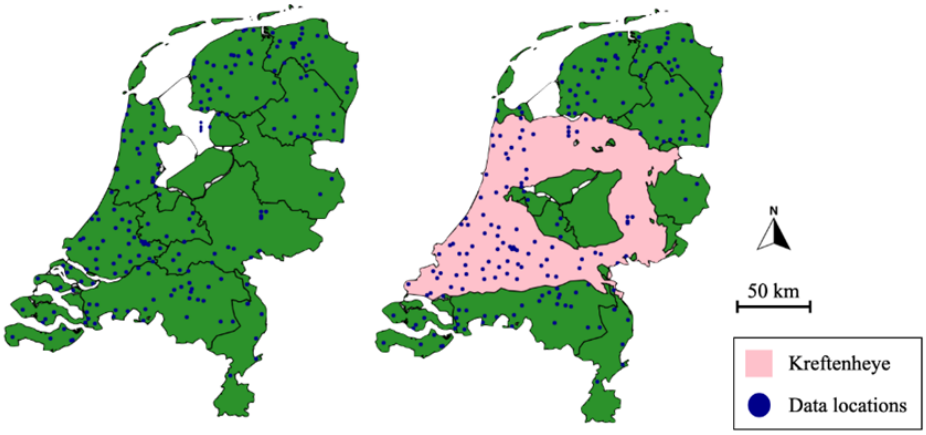

Figure 3.1: Map of the Netherlands showing the locations of the CPT and borehole pairs, including a subset of locations within the Kreftenheye Formation used in this study.

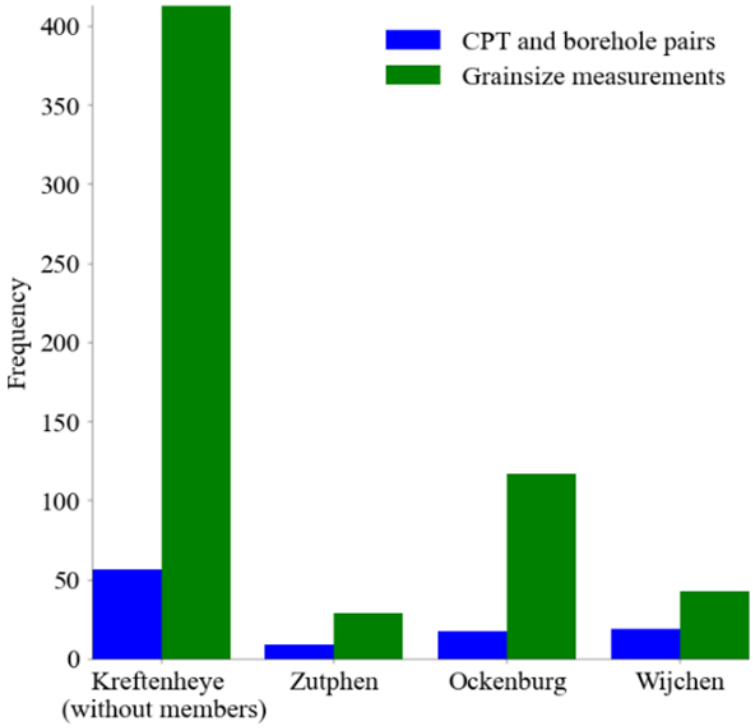

Figure 3.2: Overview of the dataset of the Kreftenheye Formation used in this study.

Figure 3.3: Map of the Netherlands showing the locations of the CPT and borehole pairs for the different members

Testing Procedures

All cores are retrieved using core drilling (*steekboring*), following Dutch standard procedures SIKB (2022) and TNO standards. This method employs a tube with sharp edges that is pushed into the soil. Once the tube is filled, it is brought to the surface, and a new tube is inserted. The process involves using an enclosed tube to stabilize the soil.

Upon retrieval, the core is documented and analyzed according to the guidelines in NEN-EN-ISO (2021). A TNO expert then interprets the core, providing a detailed description of the lithology, index tests, lithofacies, and stratigraphic units of the layers. Subsequently, the other half of the core is sampled for various measurements, including grain size analysis. Samples are collected from layers of interest within these boreholes, with the frequency of sampling varying significantly across different layers.

For the grain size analysis, particles larger than 2000 microns are first removed from the sample and weighed. The remaining sample is then analyzed using the Sympatec HELOS KR laser-diffraction particle sizer, which covers a spectrum ranging from 0.15 to 2000 microns. Furthermore, the dataset encompasses data on permeability, total porosity, wet and dry weights, geochemistry, as well as macro and trace elements derived from the samples.

Data Description

The borehole and grain size data are provided in an XLSX file, filtered based on the geological Formation of interest. The CPT data is provided in an CSV file which was retrieved from the TNO databases. All CPT data is of the quality standard class 2 (*klasse 2*) and is obtained with a $15cm^2$ cone. Tables 3.1 and 3.2 provide an overview of the most important headers in the borehole and grain size data and Table 3.3 for the CPT data.

Table 3.1: TopIntegraal locations

Header	Description
Boring_Nr	Borehole identification number
Boring_Xcrd	Borehole X coordinate (RD)
Boring_Ycrd	Borehole Y coordinate (RD)
Boring_MVm	Borehole surface level [m]
Boring_Eindem	Borehole end depth [m]
Afstand_BorSond	Distance borehole to nearest CPT
Sond_BRO_ID	CPT identification number
Sond_Xcrd	CPT X coordinate (RD)
Sond_Ycrd	CPT Y coordinate (RD)
Sond_MVm	CPT surface level [m]
Sond_Eindem	CPT end depth [m]

Table 3.2: TopIntegraal grainsize data

Header	Description
MIDDIEPTE_MONSTER	Depth mid of the sample [mm]
STRAT_DINO	Lithostratigraphy
M_D50	Grainsize D50 [μm]
M_D60/D10	Coefficient of uniformity
ZF_	Sand fractions
F0_01-0_1 to F1680-2000	Grainsize measurements
C<0_01 to C<2000	Cumulative grainsize measurements
Drooggewicht_>2mm_g	Dry weight of material larger than 2 mm [gr]

Table 3.3: TopIntegraal CPT data

Header	Description
nr	CPT number
X	CPT X coordinate (RD)
Y	CPT Y coordinate (RD
mv_cpt	CPT surface level [m]
depth_nap	Depth NAP [m]
coneresistance	Cone resistance [Mpa]
localfriction	Local friction [MPa]
frictionratio	Friction ratio [%]
porepressureu2	Pore pressure measured at u2 [MPa]

3.1.2 Visualization and Validation

Visual example of a datapoint

An example of a visual representation of all data available at a datapoint is provided in Figure 3.4. The leftmost pane displays the CPT profile over depth, illustrating the cone resistance and friction ratio. The full CPT profile is accessible at every location, and is filtered to obtain the depth intervals of interest (Kreftenheye Formation). The CPT profile offers a continuous and uninterrupted depiction of soil resistance with depth. Unlike core samples, CPT measurements cause minimal disturbance to the soil, thereby preserving in-situ conditions and providing indirect yet reliable data on soil properties.

The central left and central right panels present the grain measurements of the samples. There are eight samples available in this interval, so these measurements are not continuous and may contain gaps. The central left pane shows the grain size distribution on a logarithmic scale, represented by circles, with the circle size indicating the quantity of grains of that size. The central right panel shows the gravel content. The right panel shows the borehole lithology included in the dataset. There are numerous undetermined layers, likely due to missing or disturbed soil during the extraction process. This panel illustrates the limitations of core drilling and sampling methods, such as sample disturbance and incomplete recovery of core material.

Additional borehole pictures can be found in TNO-GSN (2024), although they are not included in the dataset. These pictures provide more detail on the sedimentary structure, highlighting the importance of boreholes compared to CPT.

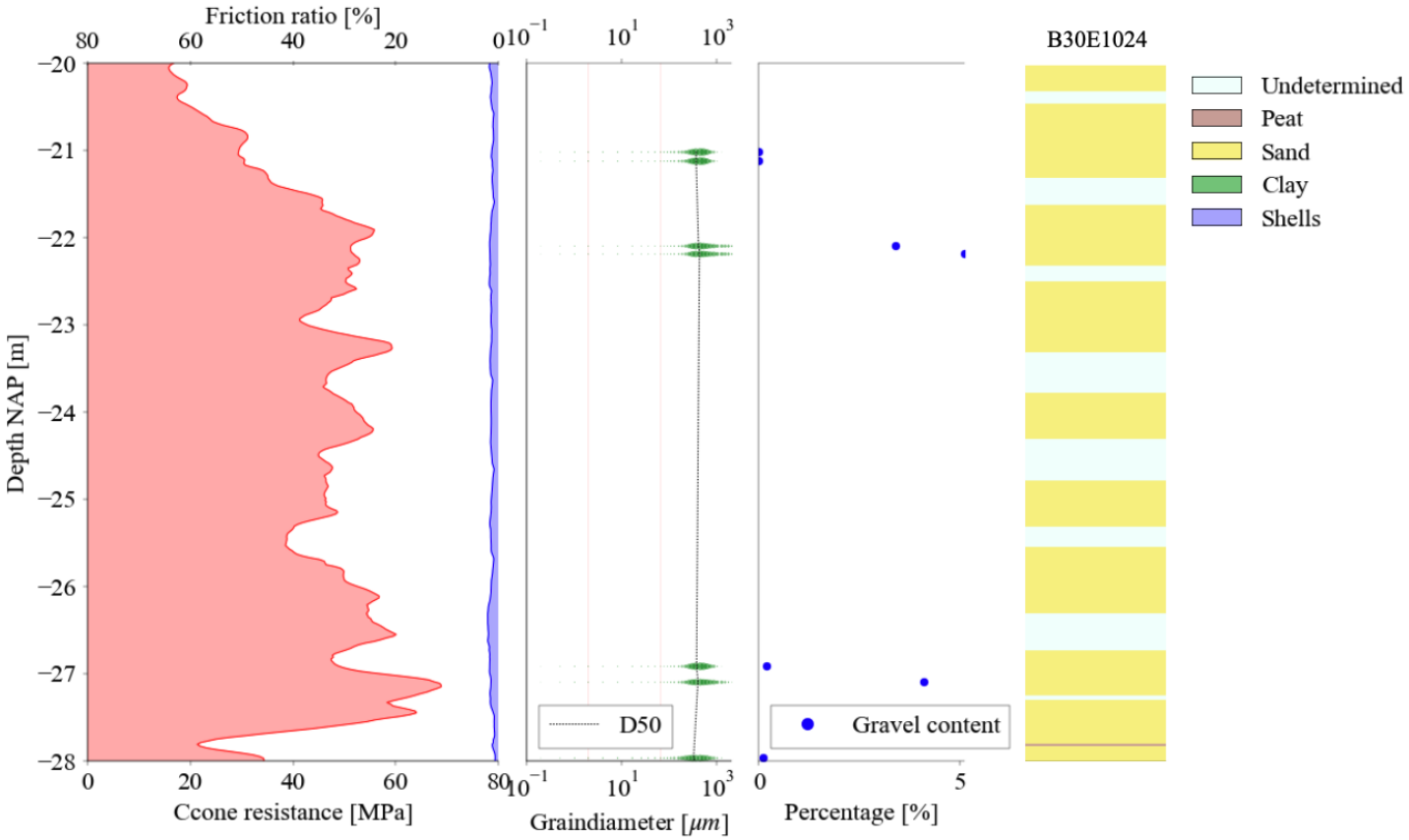

Figure 3.4: Overview of available data at one example location. Left pane: CPT measurements (CPT000000063319), left central panel: grain size measurements, central right panel: gravel content, right panel: borehole (B30E1024) lithology

Selection of CPT data

One of the challenges of this dataset is combining the correct borehole data with the CPT data while addressing the uncertainties inherent in both measurement methods.

Figure 3.5 shows a schematic diagram of how the CPT data for a layer of a formation or member is selected. In the borehole data, the layers are identified, and these layers are then linked with the CPT measurements. The top and bottom depths of a formation or member are used to define the range of CPT measurements for selection.

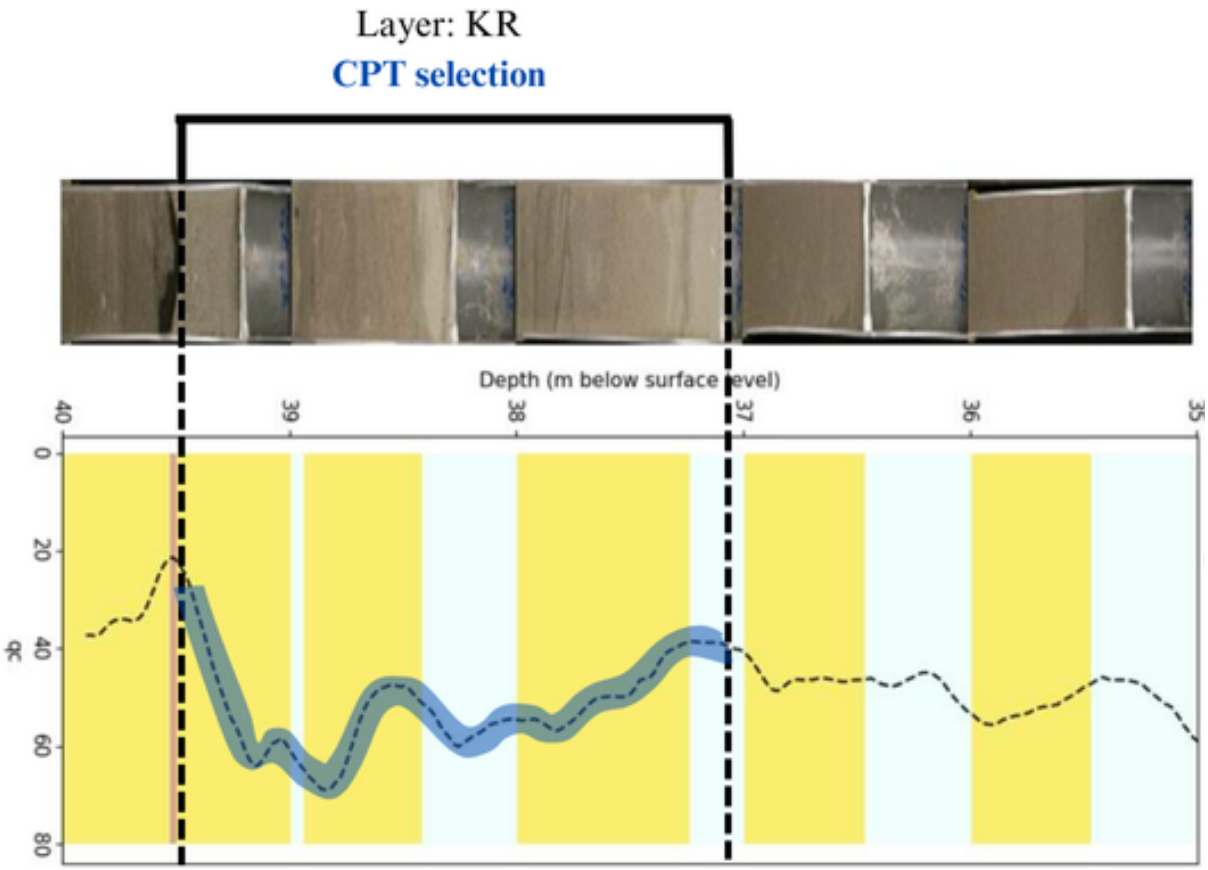

Figure 3.5: Schematic overview of combining CPT and borehole data - Layer selection

Furthermore, this study also compares grain size measurements from samples with CPT measurements. To achieve this, a more detailed selection of the CPT data is necessary. Figure 3.6 illustrates this process.

The retrieved core samples are within a range of 5-10 cm. However, the CPT selection must cover a larger range due to the accuracy and sensitivity limitations of the CPT cone. The samples were aimed to be retrieved from the middle of a layer to minimize issues related to transition zones. Considering the minimal sensing distance of a cone as discussed by Boulanger & DeJong (2018), an additional range of ±10 cm was included around the sample.

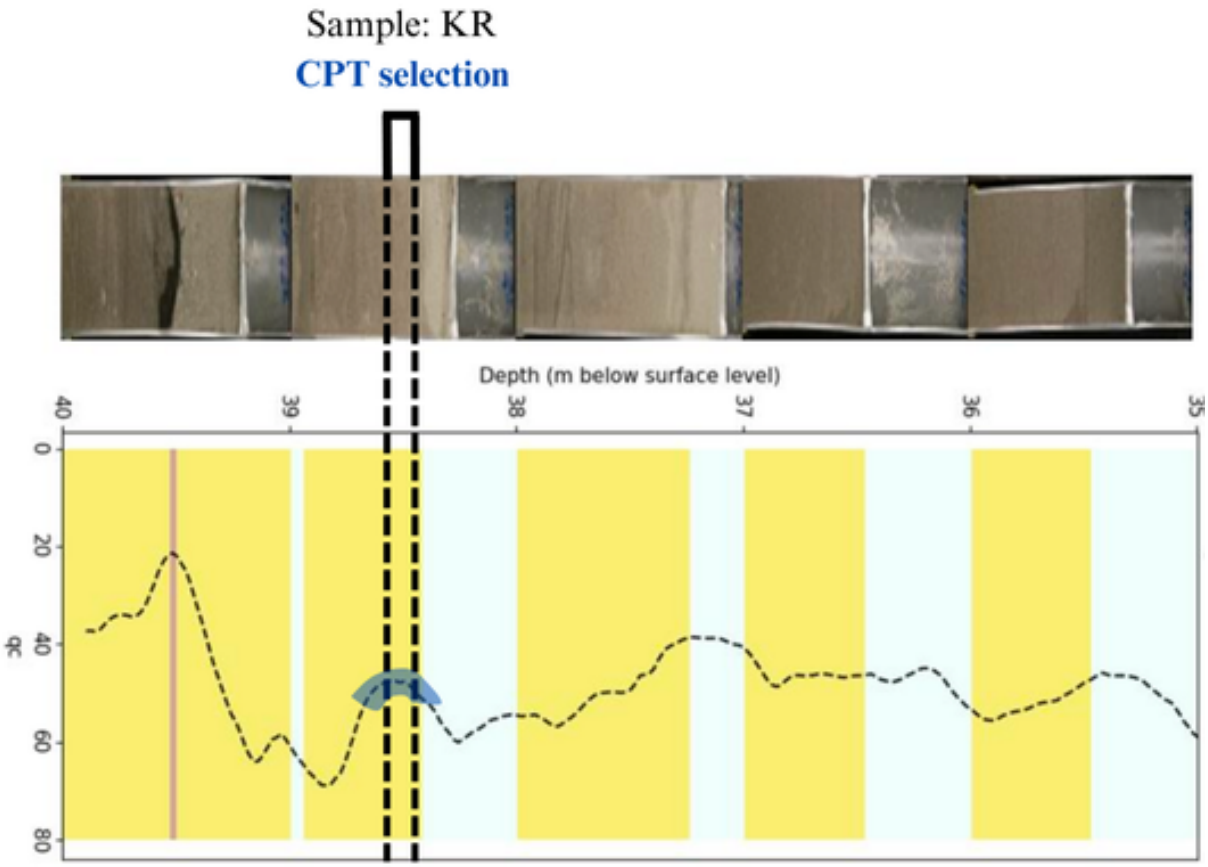

Figure 3.6: Schematic overview of combining CPT and borehole data - Sample selection. The dashed lines show the thickness of the sample and the blue highlighted line shows the selected CPT data

Local validation mutliple datapoints

To further validate and visualize the dataset, two areas were analyzed, each containing multiple data points within a 6 km distance from each other. The first area, shown in Figure 3.7, features five data points from the east of the Netherlands. The colors in the CPT profiles and grain size measurements represent different locations, with the exact locations displayed on a small map at the bottom center of the figure. The CPT profiles are quite similar, but some variations exist in the depth of the low cone resistance layer, ranging from -2 to -7 meters. This layer is also identifiable in the grain size measurements, which exhibit similar grain size distributions in this region. However, discrepancies are visible between the samples, such as the very coarse sample around -6 meters from point 4. Additionally, the grain size distributions are well-graded, showing wide ranges of grain sizes.

In Figure 3.8, a similar analysis was conducted for a location in the west of the Netherlands, with three CPTs within a 6 km distance. Here, the grain size profile is much more uniform, with consistent grain sizes over the interval. The CPT profiles, however, show variations in depths and thicknesses. Both figures indicate that a 6 km distance is quite large for comparing CPT profiles due to the variability of the subsurface. A similar conclusion can be drawn for the grain size measurements. However, there appears to be less variation in the grain size measurements in the west of the Netherlands compared to the east. This can possibly be explained by the river system, where more sorted sediments are typically found near the river's sink (west) and a

wider range of sediments near the source (east).

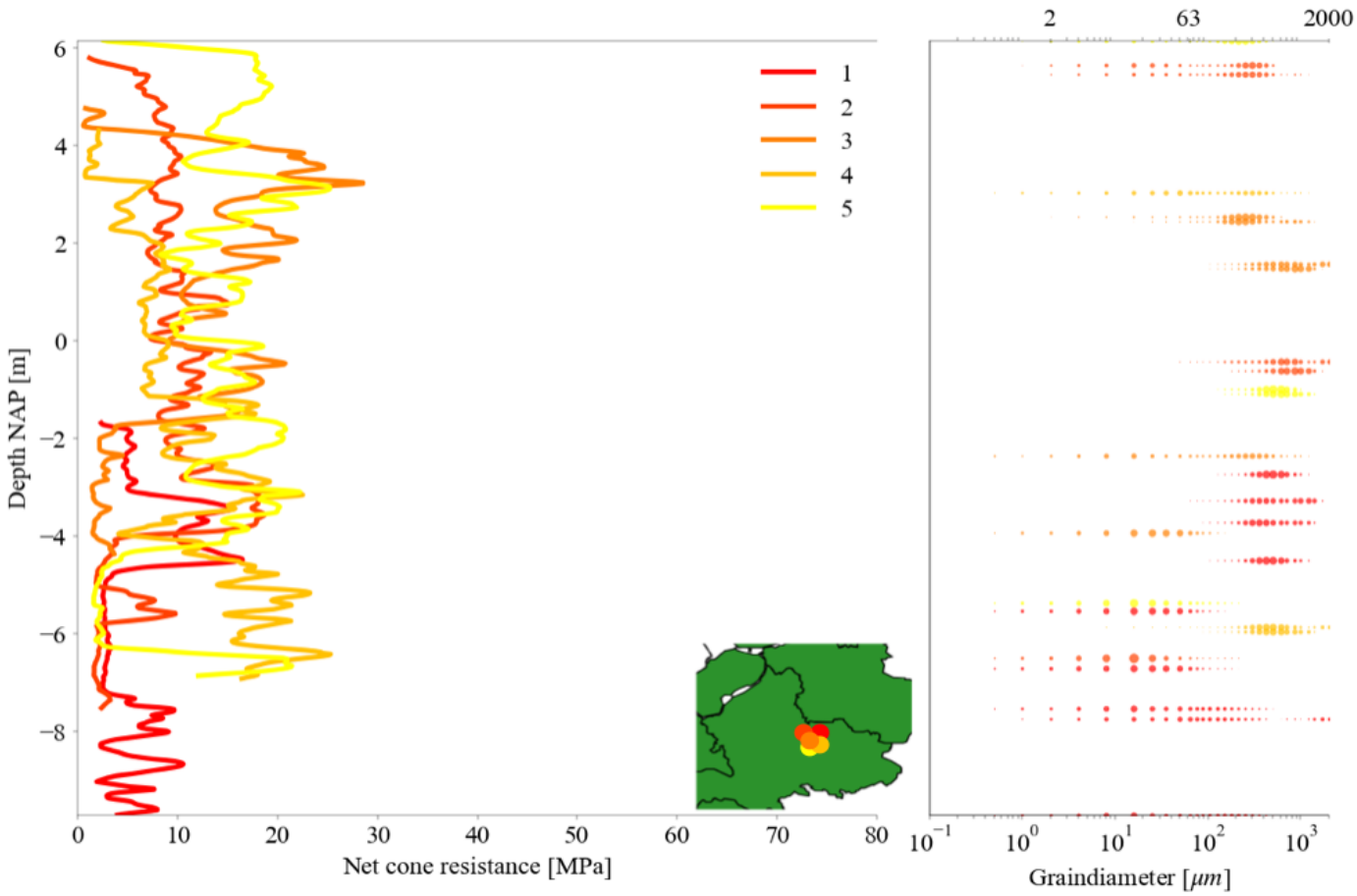

Figure 3.7: 5 CPT measurements and grain size distributions within 6 kilometre distance (CPT000000018696, CPT000000018697, CPT000000018698, CPT000000018688, CPT000000018693)

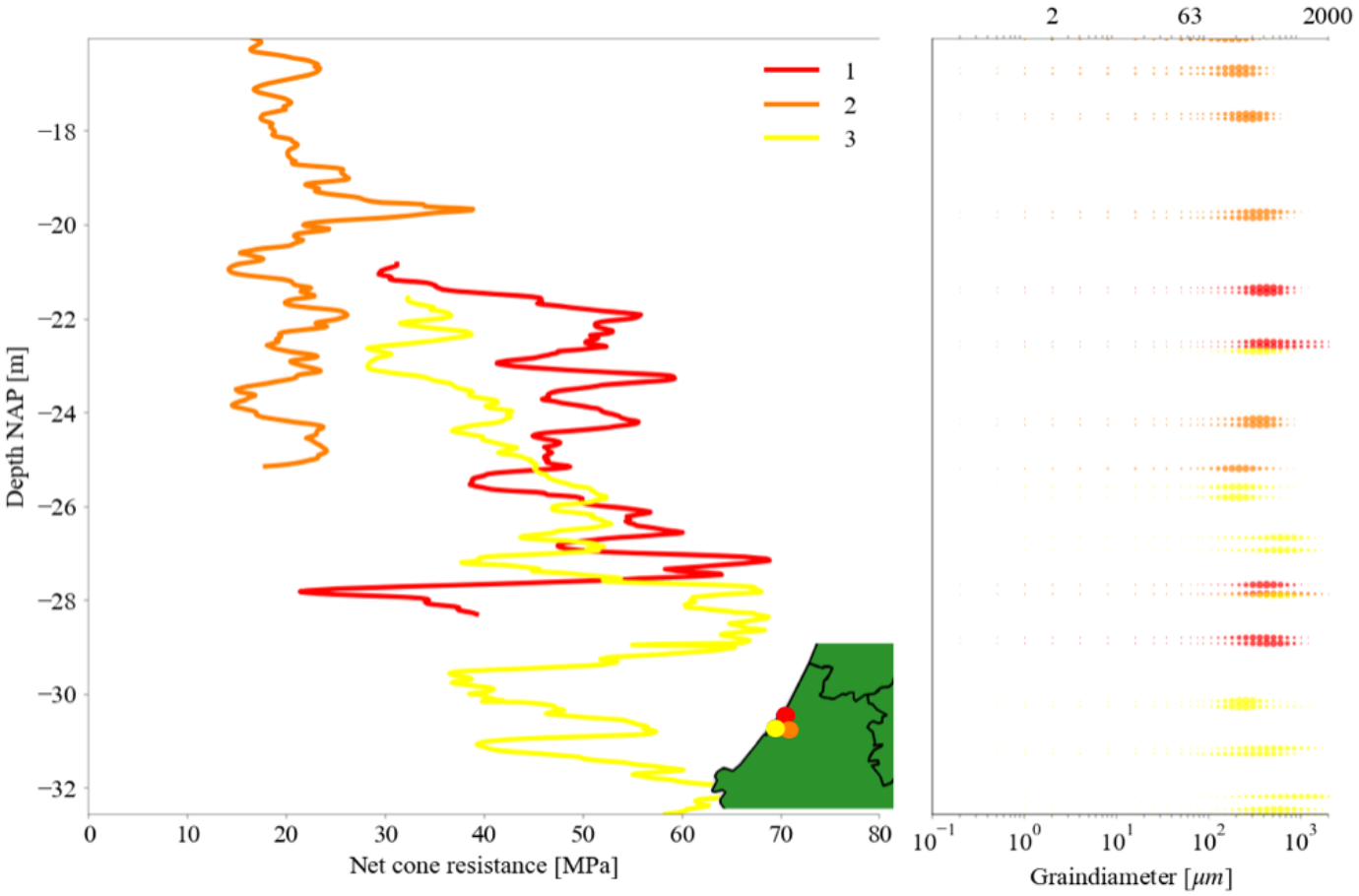

Figure 3.8: 3 CPT measurements and grain size distributions within 6 kilometre distance (CPT000000063319, CPT000000012728, CPT000000063320)

East-west validation multiple datapoints

An additional validation method used in this thesis involves analyzing trends in the data. Given that the river system serves as the depositional environment, cross-sections from east to west across the Netherlands are particularly insightful, as they may reveal patterns of sediment sorting characteristics of the river system.

Figure 3.9 presents seven locations along a line from the west to east of the southern part of Zuid-Holland. The cone resistances in this profile are quite similar, suggesting that the soil deposits may be consistent across all seven locations. However, the grain size measurements do not exhibit a clear pattern related to their distribution.

Figure 3.10 shows an analysis of seven data points over a larger distance. All CPT profiles reveal a pattern of increasing cone resistance upwards from the base of the formation, followed by a decrease. This pattern is consistent across all profiles, although some deviations are present. Such trends could indicate a similar depositional environment and river system across the locations. The grain size measurements also display similar transitions to finer materials around the zones of lower cone resistance, with no distinct differences between the grain size distributions in the eastern versus the western regions.

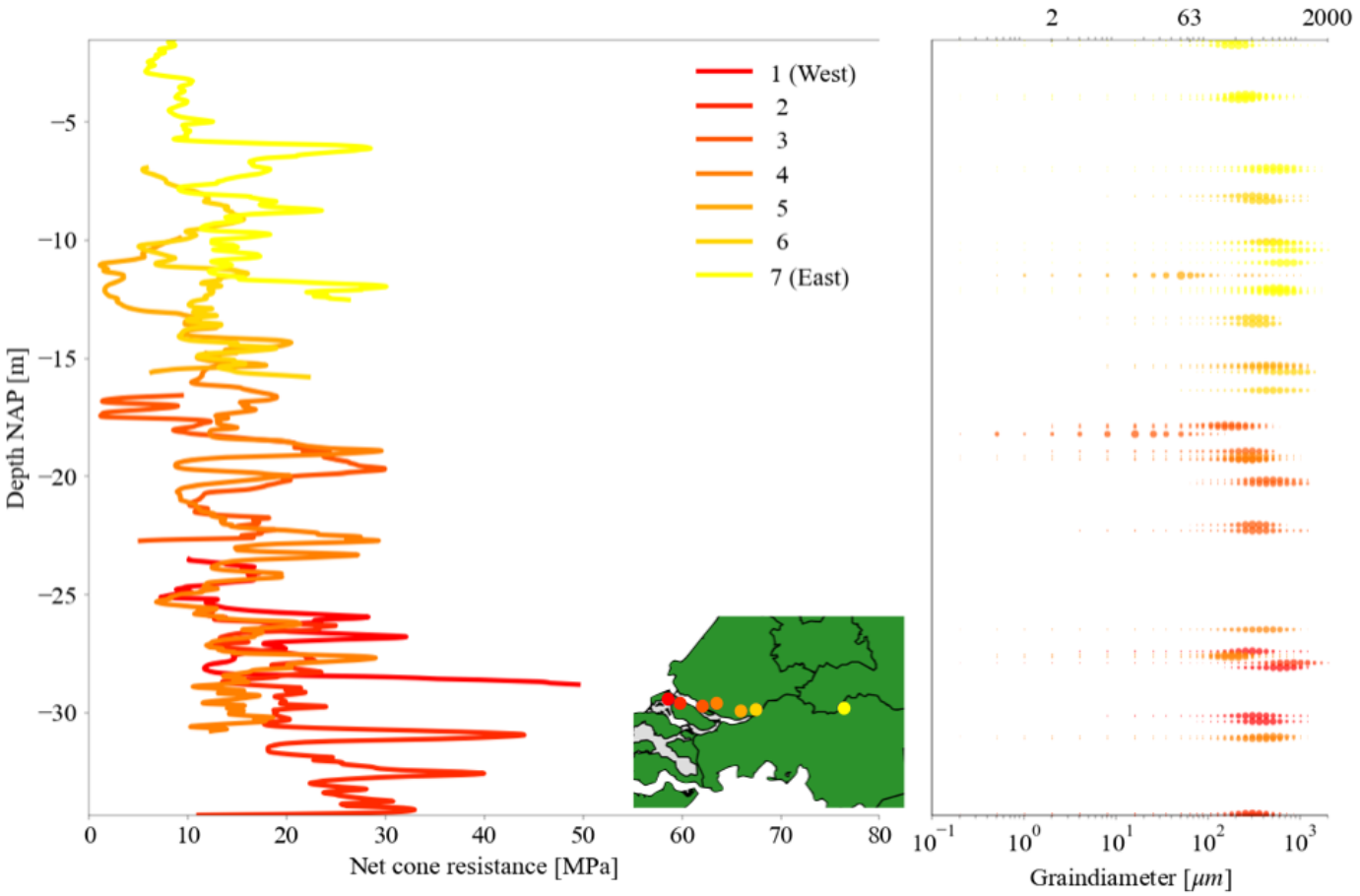

Figure 3.9: 7 CPT and grain size distributions from West to East of the Netherlands (CPT000000080417, CPT000000050619, CPT000000012733, CPT000000012732, CPT000000012744, CPT000000012741, CPT000000063344)

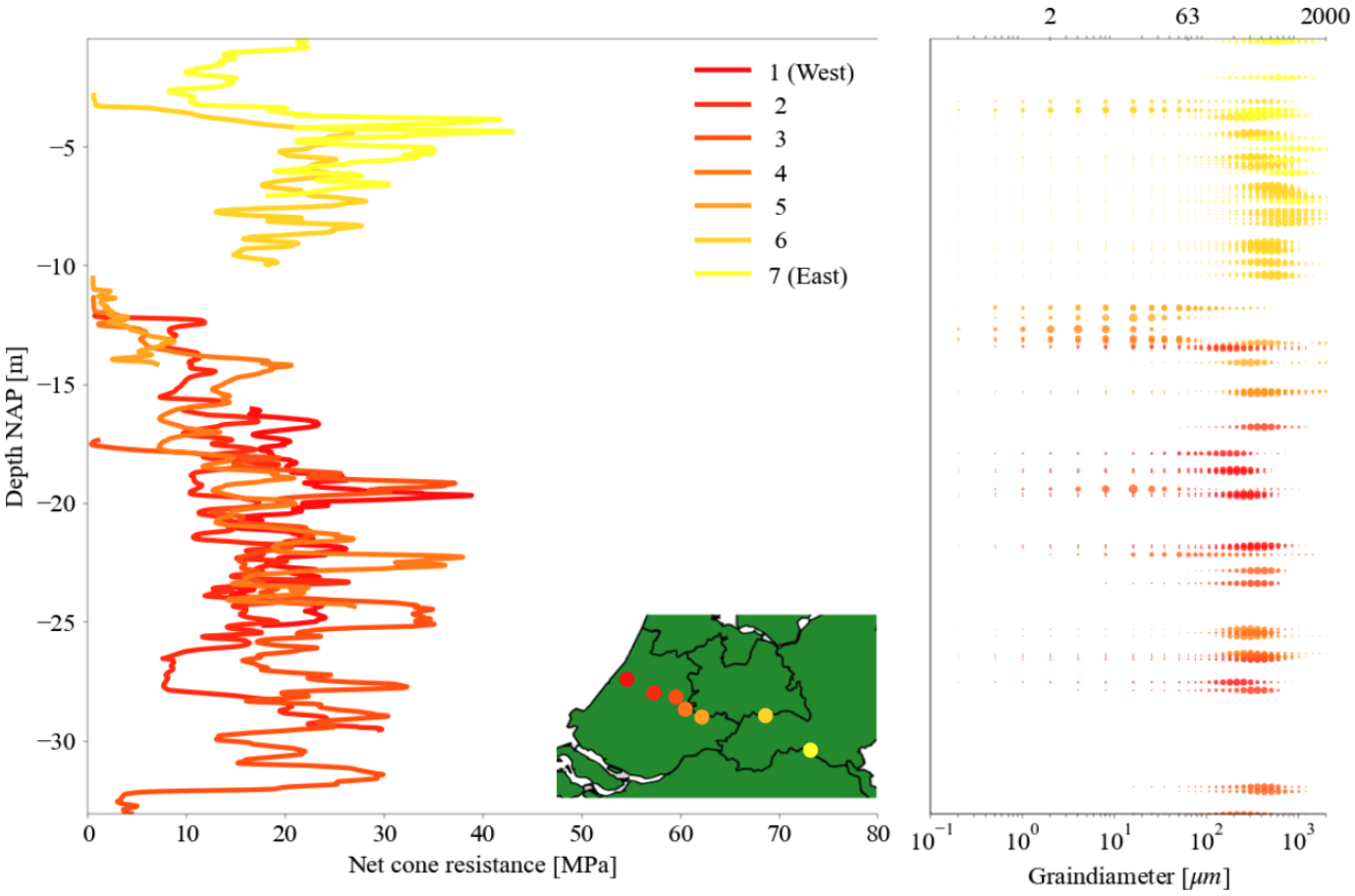

Figure 3.10: 7 CPT and grain size distributions from West to East of the Netherlands (CPT000000012728, CPT000000012751, CPT000000025396, CPT000000012737, CPT000000080414, CPT000000063329, CPT000000063332)

3.2 Boulanger and deJong (2014) CPT Filter method

3.2.1 Purpose and Use

To analyze a dataset from the Kreftenheye we need to filter the data by subdividing it into members, beds, and areas. To achieve accurate intervals for the CPT measurements, it is crucial to select data at the correct transition points between layers.

Previous studies of van den Berg (1996) and Youd & Idriss (2001) have shown that CPT measurements can be influenced by the soil conditions both ahead of and behind the cone. This influence necessitates caution when interpreting soil profiles with multiple layers, as the zone of influence around the cone can cause smoothing of measurements at layer interfaces. This zone of influence, which varies based on factors such as soil properties, penetration rate, and cone geometry, generally extends to approximately 10-30 cone diameters (Boulanger & DeJong (2018)).

In our dataset, we encounter challenges such as the soft Wijchen layer on top and the Kreftenheye sand, which complicate accurate data interpretation. Given the potential for sig-

nificant sensing distances to affect the results, we employ the Boulanger & DeJong (2018) CPT filter method to address these issues and ensure accurate and reliable data extraction. This method helps mitigate the impact of the zone of influence and improves the precision of layer transitions in our analysis.

Figure 3.11 illustrates the zone of influence schematically with three example cases, showing that when the sand layer between two clay layers becomes thinner, the 'true' cone resistance may not be accurately reflected in the CPT profile. In case $\#1$, it is evident that a transition zone is present before the 'true' cone resistance is obtained. However, in cases $\#2$ and $\#3$, although a transition zone is also present, the 'true' cone resistance is never measured. Boulanger & DeJong (2018) reviewed previous research on penetration through layered profiles and developed a filter method to achieve a more 'true' cone resistance profile.

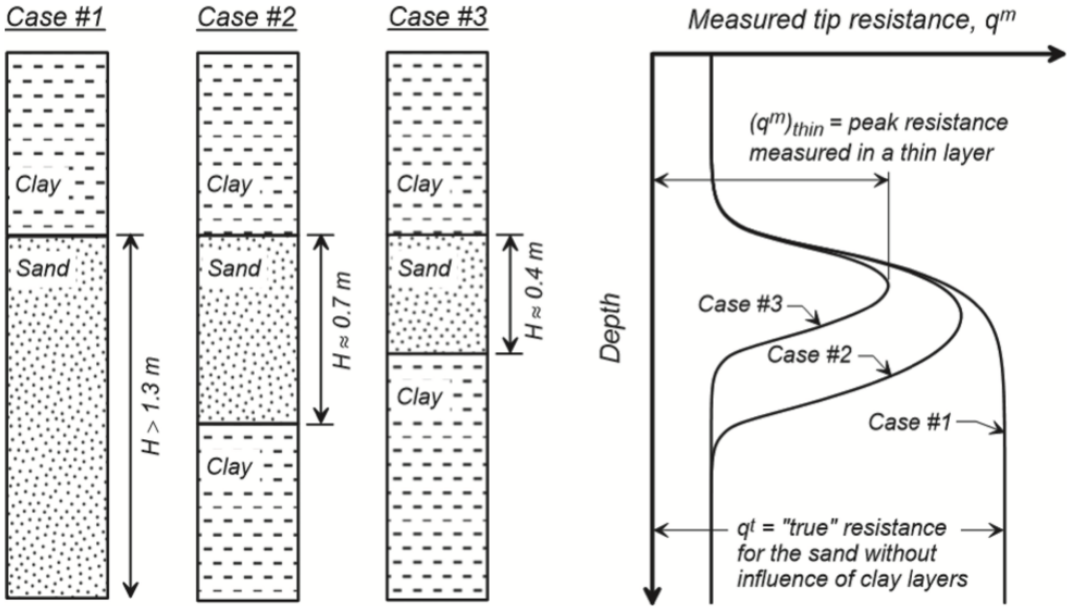

Figure 3.11: Thin layer effect (from Boulanger & DeJong (2018))

The foundation of the filter method is based on equation 3.1 where the measured cone resistance (q_m) is a convolution of the true cone resistance q_t of a soil and a weight function (low-pass filter) $w_c(z)$ that changes over distance z. This convolution can be rewritten in the form of Equation 3.2.

$$q^m(z) = q^t(z) * w_c(z) \tag{3.1}$$

$$q^m(z) = \int_{z_{min}}^{z_{max}} q^t(\tau) w_c(z - \tau) d\tau \tag{3.2}$$

The weights of the weight function (Equation 3.3) can be specified as w_1 and w_2. w_1 is a function (Equation 3.5) that assigns weights to the soil around the cone, with soil further away receiving a smaller weight, and vice versa. w_2 (Equation 3.6) represents a weight function that assigns weights based on the stiffness of the soil. Softer layers before or after the cone tip are given more weight compared to stiffer layers at the cone tip and the other way around. In these

functions, the depth is normalized by Equation 3.4 to ensure applicability across all profiles. Figure 3.12 shows a graphical representation of the weight function over the normalised depth for different cone resistance ratios.

$$w_c = \frac{w_1 w_2}{\sum w_1 w_2} \tag{3.3}$$

$$z' = \frac{z - z_{tip}}{d_c} \tag{3.4}$$

$$w_1 = \frac{C_1}{1 + (\frac{z'}{z'_{50}})^{m_z}} \tag{3.5}$$

$$w_2 = \sqrt{\frac{2}{1 + (\frac{q^t_{z'}}{q^t_{z'=0}})^{m_q}}} \tag{3.6}$$

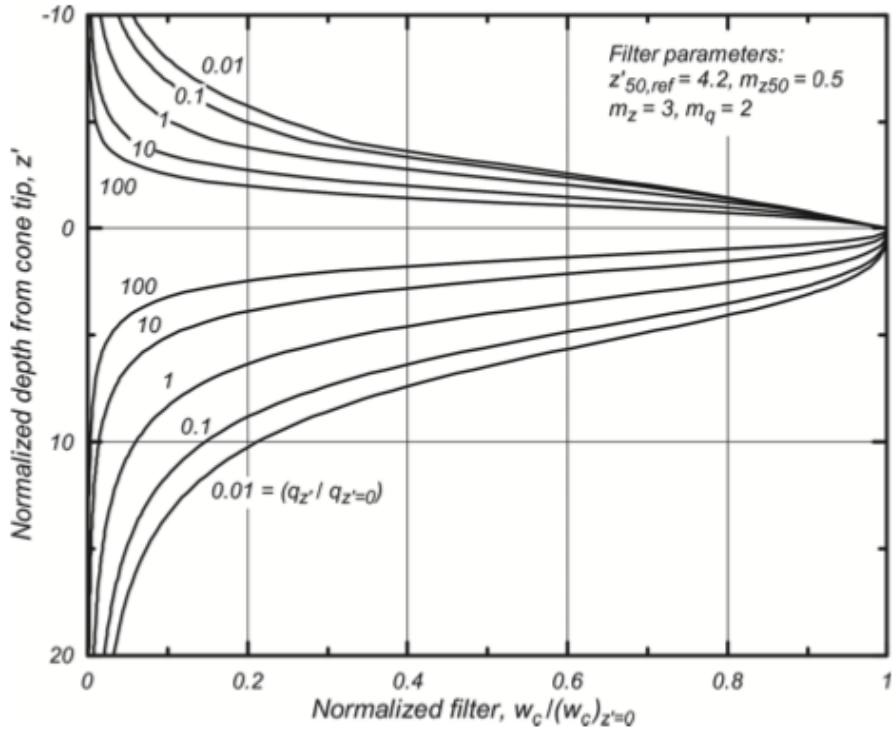

Figure 3.12: Filter method weight function (from Boulanger & DeJong (2018))

To use this method to filter data and obtain the q_t, an inversion procedure should be followed which iterates over Equation 3.7 until the error (Equation 3.8) is less than 10^{-6}. In the method, additional filters and smoothing to adjust the signal and improve the likelihood of convergence for the solution, are applied.

$$q^{inv}_{n+1} = q^m + (q^{inv}_n - q^{inv}_n * w_c) \tag{3.7}$$

$$err = \frac{\sum |(q_{n+1}^{inv} - q_n^{inv})_i|}{\sum |(q^m)_i|} < 10^{-6} \tag{3.8}$$

3.2.2 Sensitivity

This parameters of the filtering method used in this study can be calibrated for a site-specific analysis. However, due to the lack of available data for site-specific calibration, this thesis utilizes parameters obtained from Boulanger & DeJong (2018). To understand the influence of these parameters on the filtered dataset, a sensitivity analysis was performed.

The parameters investigated in this sensitivity study are:

- $z'_{50,ref}$: Adjusts variation of w_1, standard set at 4.2
- m_z: Adjusts variation of w_2, standard at 3

The sensitivity analysis evaluates the effect of varying m_q in the range of $[2, 3, 4]$ while keeping all other variables constant. The same for $z'_{50,ref}$ in the range of $[3.2, 4.2, 5.2]$ and both figures are plotted together with the measured cone resistance in Figures 3.13 and 3.14.

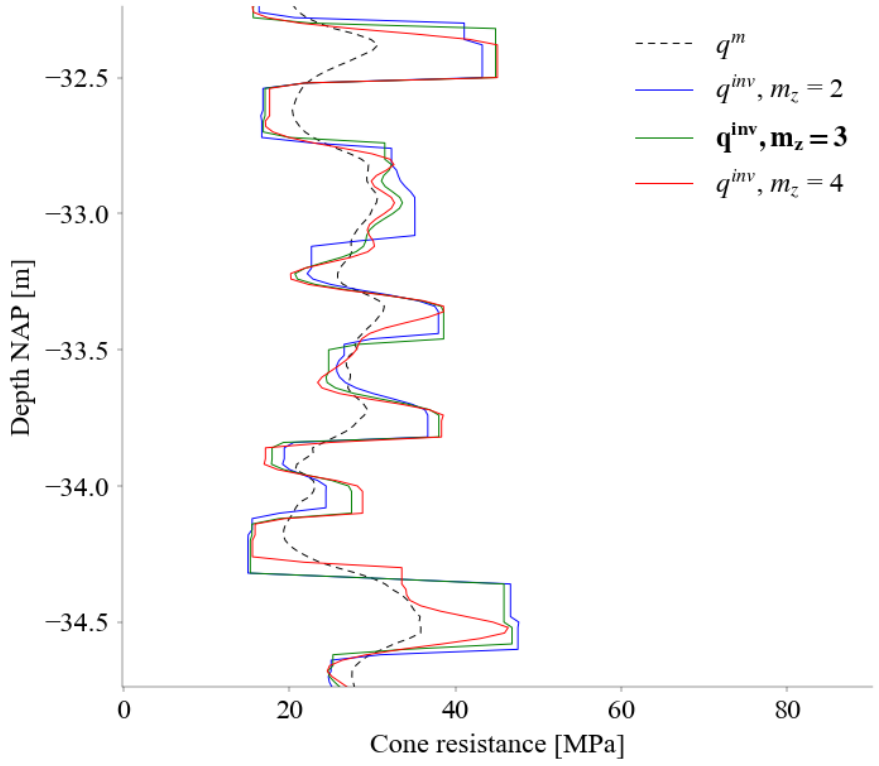

Figure 3.13: Sensitivity of m_z

From Figure 3.13, it is evident that the value of m_z significantly impacts the filtered cone resistance. As m_z increases, the variation of w_1 with z' decreases, resulting in a response that

depends on a narrower range of cone resistances. Consequently, the filtering method becomes more sensitive to thin layers. This effect is illustrated by the small peak around -34.0 m, where the red line represents the highest cone resistance values compared to the other lines. On the other hand, a lower value for m_z results in a larger range of cone resistances being included in the calculation of q^{inv}, leading to flatter peaks, such as those visible around -33 m.

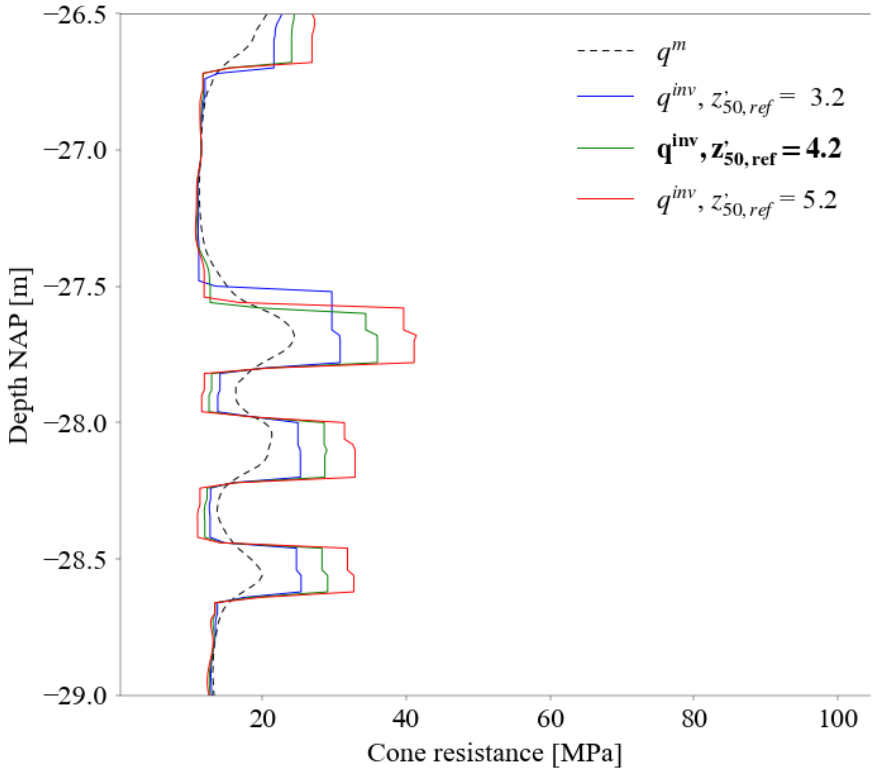

Figure 3.14: Sensitivity of $z'_{50,ref}$

In Figure 3.14, the effects of the $z'_{50,ref}$ parameter are visible. A higher value of $z'_{50,ref}$ increases the influence of the cone resistance measurements at the tip, resulting in higher cone resistance values at peaks and lower values at troughs. Conversely, a lower $z'_{50,ref}$ value reduces this influence, leading to the opposite effect.

The sensitivity study demonstrates that the parameters m_q and $z'_{50,ref}$ significantly affect the qc line and, consequently, the filtered dataset. The choice of these parameters should be made carefully, considering the specific characteristics of the study site and the objectives of the analysis. For future studies, a field calibration is recommended to refine these parameters and enhance the accuracy of the filtering method.

Due to the unavailability of site-specific data, further calibration could not be performed in this study. However, the sensitivity analysis provides valuable insights into the robustness of the method and highlights the importance of parameter selection in achieving reliable results.

Chapter 4

Results and Discussion

The Kreftenheye Formation holds significant importance due to its relevance as a foundational layer influencing pile response, drivability, and the stability of sheet piles, as well as its impact on groundwater dynamics. Understanding the extent, variability, and geotechnical characteristics of this formation is crucial for various engineering applications. The database analysis in this thesis aids in this understanding. The unique combination of CPT and borehole data in the database presents a rare opportunity to merge geological and geotechnical knowledge, which is particularly pertinent for ground modeling applications.

The Results and Discussion chapter begins with an overview of data for the Kreftenheye Formation, including its members and beds, and evaluates how well these fit within the geological context established in the literature review.

The second section of the chapter identifies spatial trends and patterns within the data, which are essential for effectively modeling the formation. For example, the differences between Area A and Area B are analyzed to determine if they should be modeled separately. Additionally, a detailed examination of the Ockenburg Member and its characteristics is presented. Lastly, spatial cross-sections of the CPT data are compared with cross-sections from the literature.

The third and final section of the chapter focuses on more local features identified in the boreholes, underscoring their importance in dataset interpretations in future research and engineering applications. These include the sensing distance with the Wijchen Bed on top of the Kreftenheye and weak zones within the Kreftenheye Formation, emphasizing their spatial variability, extent, origin, and associated uncertainties.

For optimal database analysis, all CPT profiles were filtered using the method described by Boulanger & DeJong (2018). This approach allows for deeper insights into the formation's characteristics by removing transition zones.

4.1 General Kreftenheye Formation Analysis

Kreftenheye Formation

From the literature review, the Kreftenheye Formation is identified as a sand deposit that formed over an extended period under varying climatic conditions. Consequently, a wide range of grain sizes and cone resistances is expected within the dataset.

Figure 4.1 provides an overview of the CPT and grain size data for the undifferentiated Kreftenheye Formation. The histogram of cone resistance in Figure 4.1a reveals a right-skewed

distribution with an approximate mean of 16 MPa. The 95 % confidence interval ranges from 4 to 28 MPa. The lower end of this range, 4 MPa, is relatively low for sand, suggesting that a significant portion of the Kreftenheye Formation may not be purely sand. This can be attributed to the climatic conditions during the Eemian and late Weichselian periods, characterized by warmer temperatures and slow meandering river systems, which facilitated the deposition of finer sand and clay particles.

The grain size distribution depicted in Figure 4.1b shows that a considerable number of samples (indicated by lines in the graph) have higher proportions of clay and silt. This variability in grain size confirms that the Kreftenheye Formation is not a uniform soil. Thus, caution is warranted in engineering design, as the formation exhibits a substantial variation in both cone resistance and grain sizes.

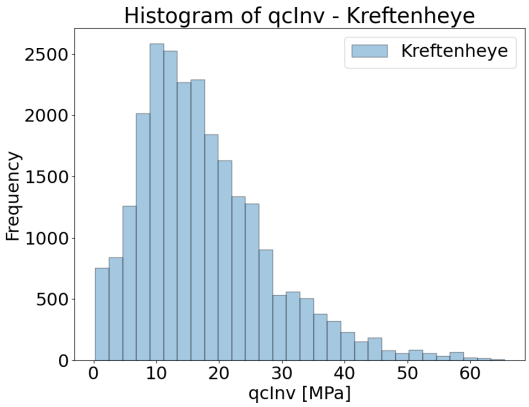

(a) 4.1.a Kreftenheye (Histogram)

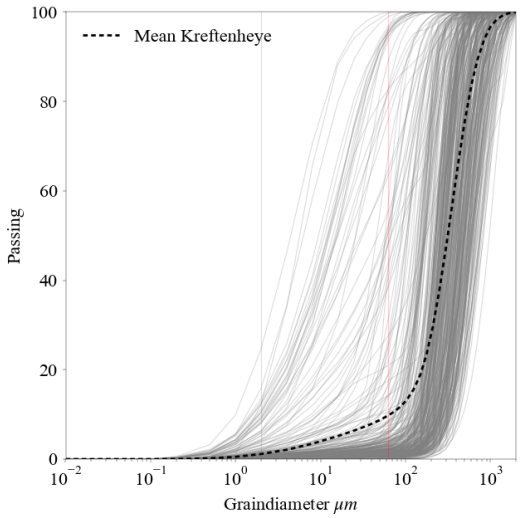

(b) 4.2.a Kreftenheye (Grain Size)

Figure 4.1: Histogram of filtered q_c measurements and cumulative grain size distribution plot for the (undifferentiated) Kreftenheye Formation

Zutphen Member

The Zutphen Member, as described in the literature review, is characterized by sediments typical of a meandering river system. In such environments, fine-grained silts and clay tend to accumulate in the river's central areas, while sand collects along the riverbanks. Consequently, it is expected that the Zutphen Member displays a range of grain sizes and variable CPT responses.

Figure 4.2a shows the histogram of cone resistances for the Zutphen Member (highlighted in orange). The distribution predominantly features low q_c values and reveals a slight bimodal pattern, with peaks representing more sandy soils (around 15 MPa) and clay/silt soils (around 2 MPa). This bimodal distribution aligns with expectations outlined in the literature review. It is also noteworthy that the Zutphen distribution contains significantly fewer data points compared to the Kreftenheye distribution.

The cumulative grain size distribution for the Zutphen Member, illustrated in blue in Figure 4.2b, displays well-graded sand, silt, and clay, along with some gap-graded distributions. This

distribution confirms the depositional environment described in the literature review, reflecting the anticipated variation in grain sizes.

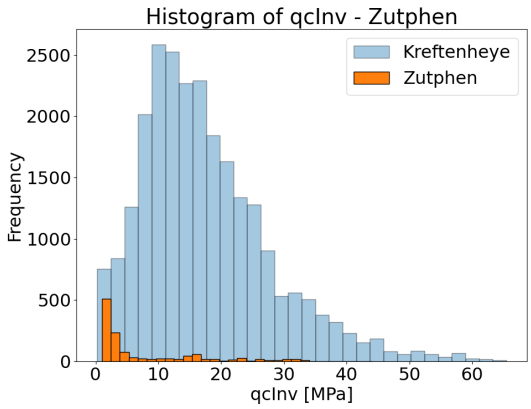

(a) 4.1.b Zutphen (Histogram)

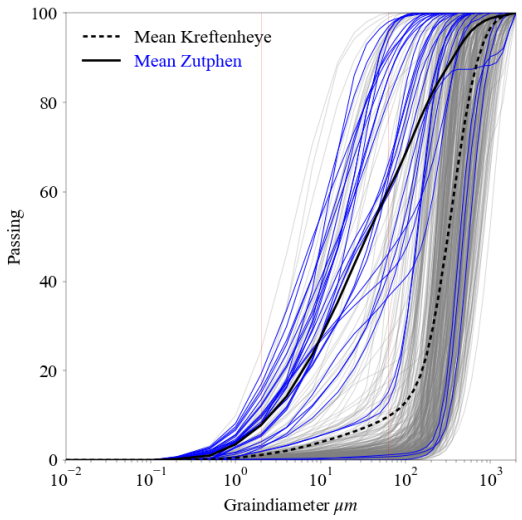

(b) 4.2.b Zutphen (Grain Size)

Figure 4.2: Histogram of filtered q_c measurements and cumulative grain size distribution plot for the Zutphen Member

Ockenburg Member

For the Ockenburg Member, the literature review highlighted the presence of a highly energetic braided river system, characterized by local features such as fining upward sequences, reworked marine sediments, and possible channel lag.

In the CPT histogram shown in Figure 4.3a, a wide distribution of cone resistances is evident in orange. The mean cone resistance of the Ockenburg Member is 26 MPa, significantly higher than the mean of the Kreftenheye Formation. Additionally, there are many more high cone resistance measurements compared to the Kreftenheye. These higher cone resistances may be attributed to the energetic braided river system, which deposits coarse-grained sand and gravel. Another possible cause is the cementation of carbonate in reworked marine fossils, which increases soil strength (Fukue et al. (1999)). Further research is recommended to determine the exact causes of the high cone resistances, specifically through a detailed study of the calcium carbonate content of the samples.

Figure 4.3b displays the cumulative grain size distribution for the Ockenburg Member, indicating a predominantly coarse, uniformly graded soil, with some outliers containing smaller grains.

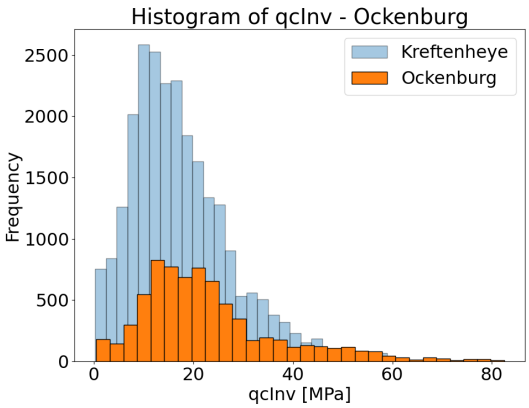

(a) 4.1.c Ockenburg (Histogram)

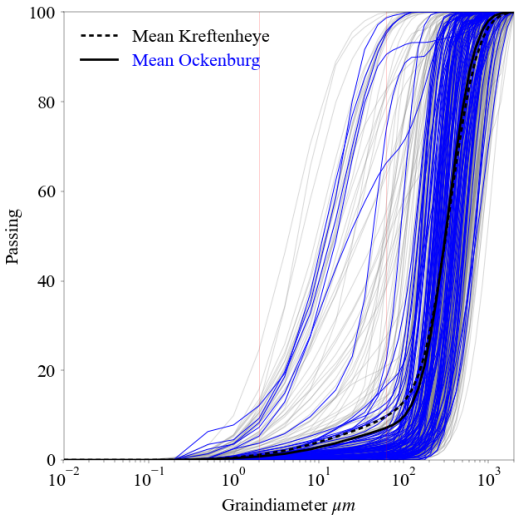

(b) 4.2.c Ockenburg (Grain Size)

Figure 4.3: Histogram of filtered q_c measurements and cumulative grain size distribution plot for the Ockenburg Member

Wijchen Bed

The final examined is the Wijchen Bed, composed of clay sediments from meandering river systems, along with some wind-blown fine-grained sand. These two soil types are clearly distinguishable in the cumulative grain size distribution in Figure 4.4b. This plot shows multiple lines with a gap-graded distribution, indicating the presence of both clay and wind-blown sand in the Wijchen Bed. Additionally, uniformly graded clay and silt samples are visible in the distribution, representing deposits from the middle of the river.

Subfigure 4.4a zooms in on the Wijchen distribution in orange, highlighting the limited amount of cone resistance data available for this member. The distribution is right-skewed and exhibits a low mean of 0.8 MPa, with a very narrow 95% confidence interval.

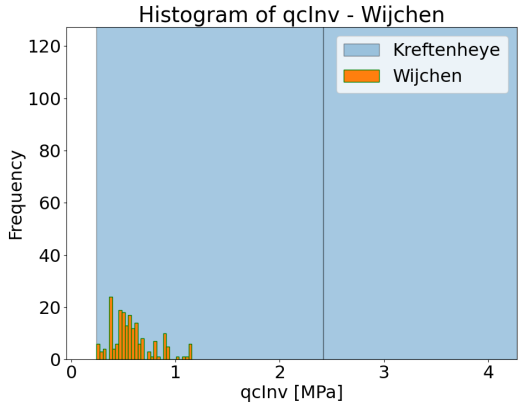

(a) 4.1.d Wijchen (Histogram)

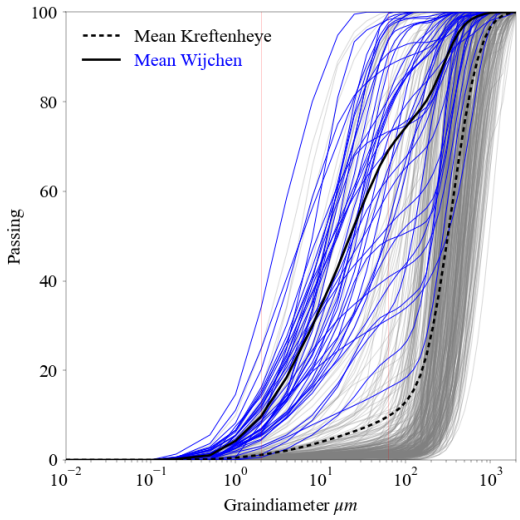

(b) 4.2.d Wijchen (Grain Size)

Figure 4.4: Histogram of filtered q_c measurements and cumulative grain size distribution plot for the Wijchen Member

4.2 Area A and B

Adetailed analysis conducted in this Thesis focuses on identifying differences between two regions within the Kreftenheye Formation. According to Busschers (2008), the Kreftenheye Formation can be divided into two distinct areas based on region and age: Area A, the upper/northern branch of the river system, deposited during the Weichselian and Eemian periods, and Area B, the lower/southern branch of the river system, deposited during the Saalian and Weichselian glacial periods. Busschers (2008) distinguished these areas using continuous core samples; however, a detailed analysis based on Cone Penetration Test (CPT) measurements has not yet been conducted.

From a geotechnical engineering perspective, distinguishing between these two areas is crucial for accurately modeling the Kreftenheye Formation. Stratigraphic changes within the Kreftenheye Formation can significantly affect how the formation is modeled at both site-specific and regional levels. CPT-based ground models are used to infer soil properties between investigation points and, in the context of deep sand formations, are essential for both stochastic and probabilistic modeling of deep excavations (Roubos (2019)) as well as for offshore and onshore piled foundations (Peuchen et al. (2022); Vanneste et al. (2022)).

Figure 4.5 presents the CPT data for the undifferentiated Kreftenheye Formation, excluding the members, categorized into Areas A and B, and plotted on a Robertson (1990) classification chart for translating CPT soundings into soil types. The plot reveals significant differences between the regions: Area A exhibits a wider range of cone resistances and friction ratios compared to Area B, with Area A having a higher proportion of low cone resistance soils. Additionally, the grain size distribution plot for Areas A and B shows a similar pattern, with Area B comprising more uniform and coarser material compared to the more variable and fine-grained material in Area A.

These depositional and sedimentological differences have important geotechnical implications. For example, the coarser and more uniform sediments in Area B may indicate higher bearing capacities and lower compressibility, making it a potentially more stable foundation for construction. In contrast, the more varied grain size distribution in Area A suggests a different set of geotechnical properties, with potentially lower bearing capacities and higher compressibility due to the presence of finer sediments. The coarser and more uniform sediments in Area B can be attributed to the colder climate and low vegetation of the Saalian glacial period compared to the more variable Weichselian period (Peeters et al. (2015)). These conditions contributed to a more energetic river system, which deposited coarser and more uniform sediments.

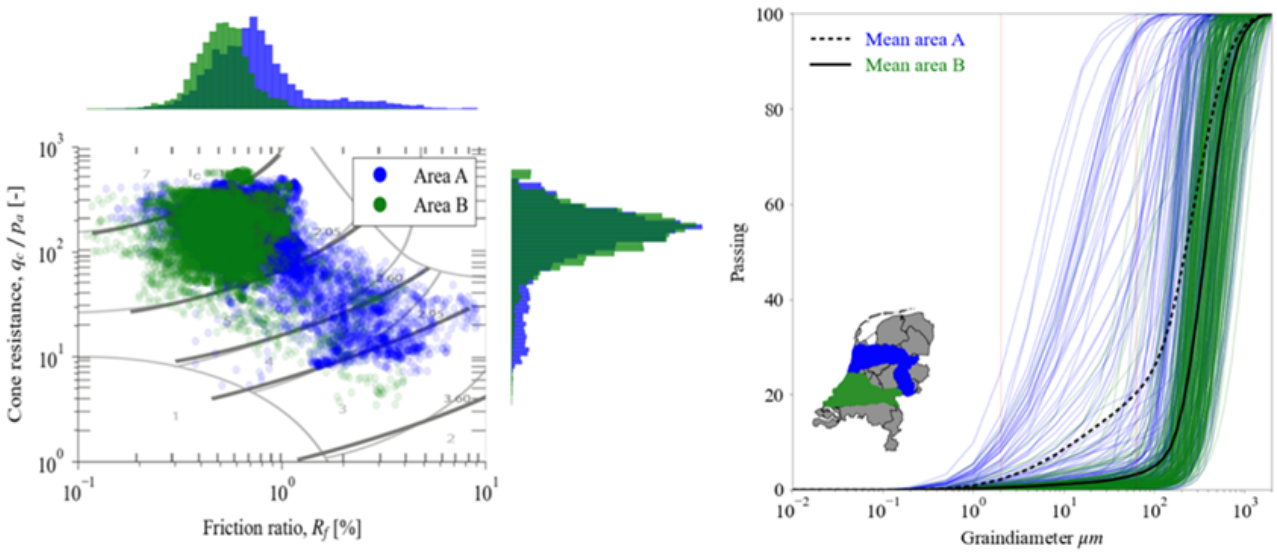

Figure 4.5: Robertson (1990) soil classification chart and the cumulative grain size distribution for Areas A and B of the undifferentiated Kreftenheye Formation. 27 CPTs and 157 grain size distributions for Area A, 26 CPTs and 256 grain size distributions for Area B

To better distinguish between Area A and Area B from a geotechnical engineering perspective, rather than from a geological standpoint, additional variables were analyzed to highlight the necessity of modeling these areas separately in a ground model. Figure 4.6 illustrates the gravel content in both areas, showing that Area B contains a higher percentage of gravel compared to Area A. This confirms the presence of coarser sediments and a higher energy river system in Area B, as previously described.

To further compare the two areas, the vertical scale of fluctuation was examined. The data was not detrended because it was stationary; this was confirmed through analysis. The vertical scale of fluctuation was determined using autocorrelation functions, most of which followed a cosine exponential model (Onyejekwe et al. (2016)). The scales of fluctuation were found to be very similar for both areas, as shown in Figure 4.7 and Table 4.1.

In conclusion, the observed differences underscore the importance of considering these areas separately in geotechnical analysis and modeling. Further research is recommended to identify additional differences between the two areas, such as variations in grain shape and mineralogy.

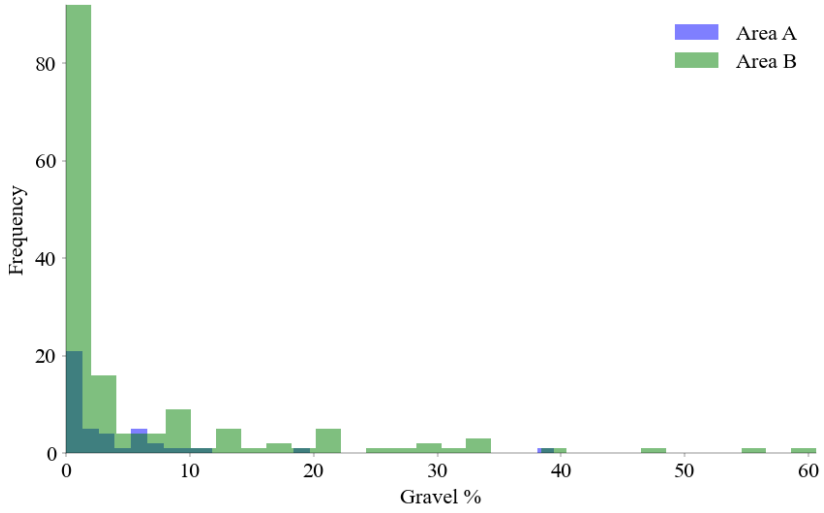

Figure 4.6: Gravel Percentage of Area A and B

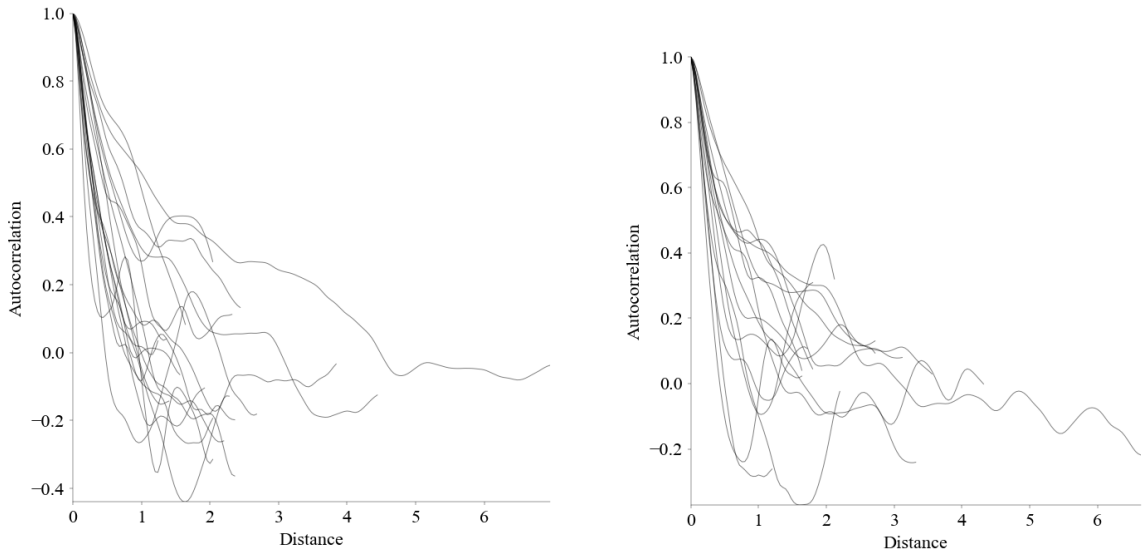

(a) Area A

(b) Area B

Figure 4.7: Autocorrelation functions

Table 4.1: Vertical scale of fluctuation

	Area A	**Area B**
Theta opt	0.95 m	1.04 m
Theta cov	0.00155	0.00149

4.3 Borehole Features and Local Geological Characteristics

The upcoming detailed analysis of local features utilizes the unfiltered CPT data to highlight the sensing distance and the influence of weak layers at a local level. In this context, filtering is deliberately avoided, as it could remove critical details relevant to understanding the interaction of weak layers with the soil profile. This approach is distinct from the previous large dataset analysis, where filtering was beneficial for generalizing trends and patterns. By preserving the unfiltered data, this analysis aims to provide a more nuanced view of the localized variations and their impact on geotechnical assessments.

4.3.1 Sensing distance Wijchen Bed

As detailed in the Methodology chapter of this thesis, as well as in laboratory research by Ahmadi & Robertson (2005), de Lange (2018), and Tehrani et al. (2018), and numerical studies by Van den Berg (1994), it has been established that CPT tip resistance is influenced not only by the soil directly at the tip but also by the surrounding soil in a zone extending several diameters above and below the CPT tip.

Figure 4.8 illustrates this effect in a field measurement context, specifically within the Wijchen Bed, which is approximately 25 cm thick and overlying the Kreftenheye Formation. In the borehole picture, the transition zone is marked by a red circle. The CPT data initially identifies the presence of the Wijchen Bed, and the subsequent transition to the underlying Kreftenheye Formation is characterized by a noticeable increase in cone resistance. This transition extends over a vertical range of more than a quarter of a meter, suggesting that the influence of the overlying soil affects a significant depth of the CPT tip resistance.

The extended transition observed is unlikely to result from a gradual mixing of clay and sand over such a distance within the Wijchen Bed, given its distinct depositional environment compared to the Kreftenheye Formation sand. This observation indicates that the CPT cone is influenced by the Wijchen Bed even after it has physically passed through its boundary, due to the sensing distance.

Therefore, this finding underscores the importance of considering the sensing distance when interpreting CPT data, particularly in the initial interval of the Kreftenheye Formation. It highlights the need for using filtering methods when analyzing large datasets of formations and emphasizes the necessity of accounting for this phenomenon when calculating the bearing capacity of piles from CPT profiles.

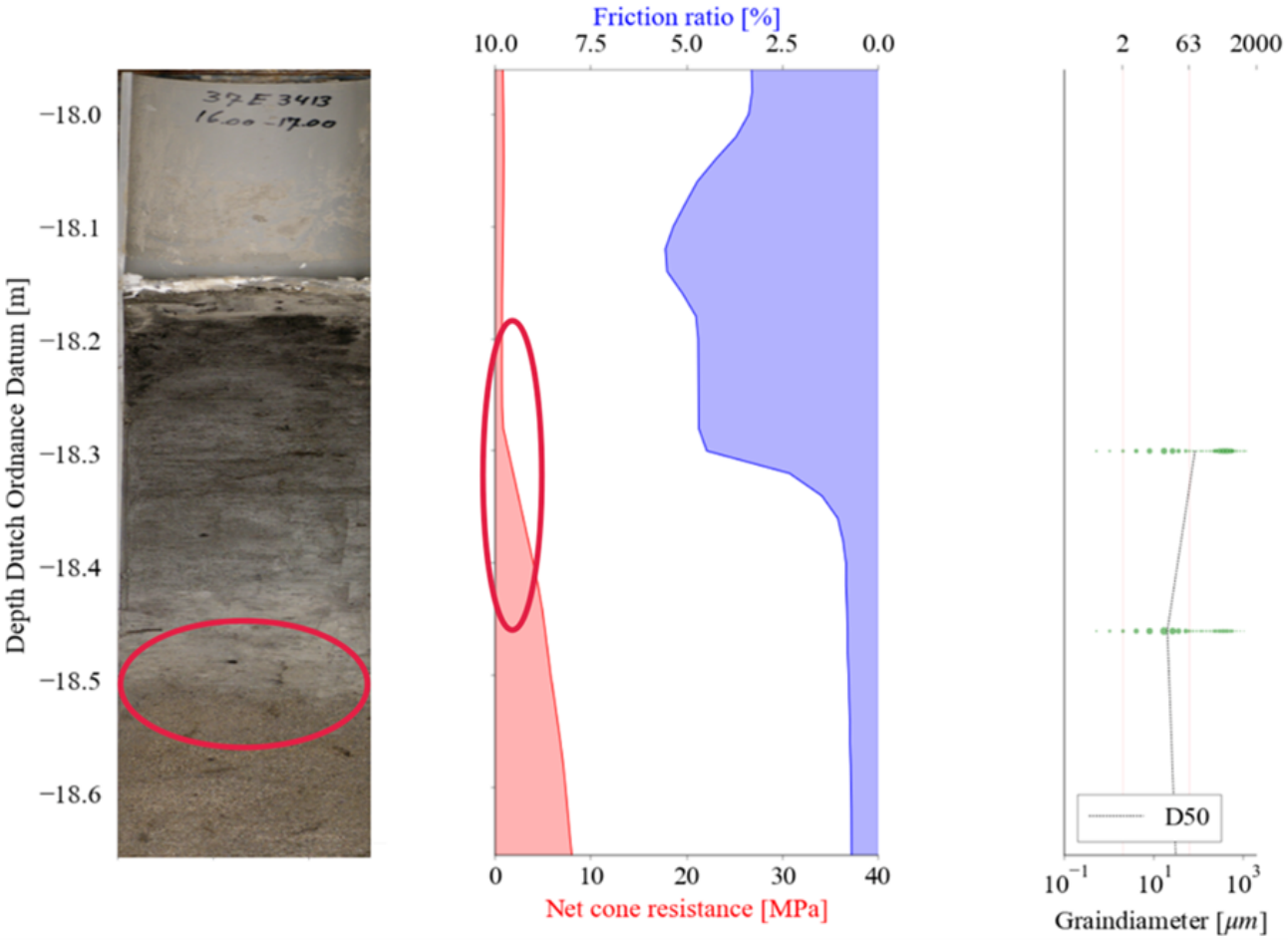

Figure 4.8: Influence of sensing distance on the Wijchen Bed. Left pane: photo taken from the borehole (B37E3413), central panel: CPT of the same interval (CPT000000012746), right panel: grainsize measurements for the interval

4.3.2 Weak zones within the Formation

Interlayered floodplain or soft channel lag deposits occur within the undifferentiated fluvial Kreftenheye Formation and can significantly affect the response of foundation piles, as studied by Chai & Tehrani (2022). Their research underscores the importance of identifying weak zones and understanding their extent. Figure 4.9 illustrates an example of an intermediate weak zone in the CPT response within the undifferentiated Kreftenheye Formation, indicated by a red circle. However, the borehole picture shows no clear weak zone that can be linked to the CPT response. In other borehole pictures, small clay pebbles are visible, indicating that channel lag deposits described by Busschers (2008) may be present, and it is possible the CPT cone encountered one.

The discrepancy between CPT data and visual soil observations underscores the need to integrate geological context with CPT data interpretation. While CPT provides valuable insights into soil behavior, it may not always detect the physical presence of weak zones such as channel lag deposits. This integration is crucial because relying solely on CPT data without considering the geological setting can lead to an incomplete understanding of soil conditions, affecting the

assessment of bearing capacity and settlement of foundation piles. Such oversight could result in overestimations or underestimations of foundation performance. Therefore, incorporating detailed geological surveys alongside CPT data is essential for obtaining a comprehensive view of subsurface conditions, ensuring that the impact of weak zones on foundation stability is accurately assessed and managed in engineering design.

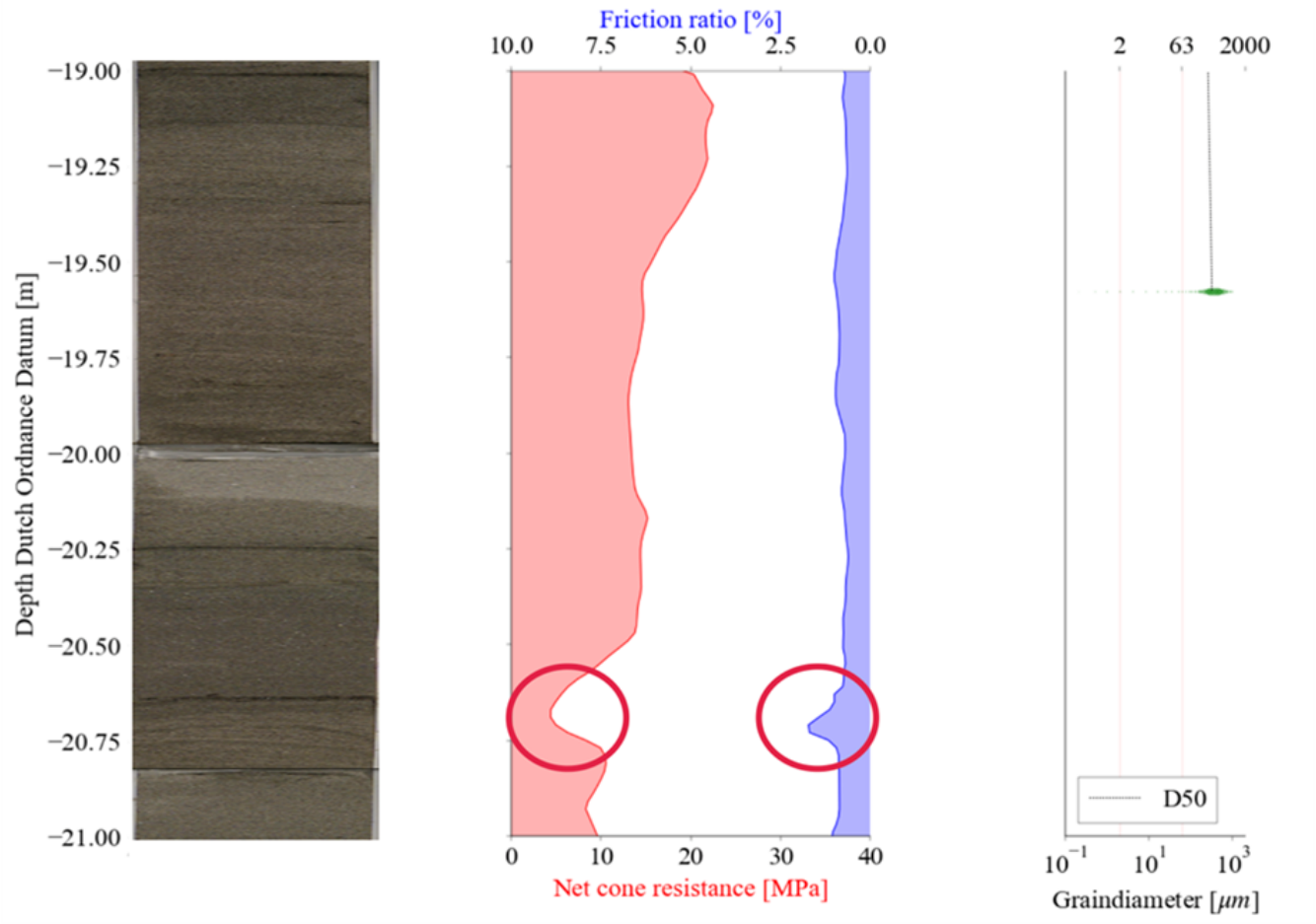

Figure 4.9: Intermediate soft layer within the Kreftenheye Formation. Left pane: photo taken from the borehole (B14E0952), central panel: CPT of the same interval (CPT000000043211), right panel: grainsize measurements for the interval

Chapter 5

Conclusion and Recommendations

Understanding the geological and geotechnical characteristics of the Kreftenheye Formation is vital for making informed engineering decisions in the Netherlands, where this formation significantly impacts foundation design and groundwater management. This thesis provides a thorough analysis of the Kreftenheye Formation, using a unique dataset comprising nearly 200 Cone Penetration Tests and borehole pairs, complemented by detailed grain size measurements and various laboratory tests.

The analysis offers valuable insights into the formation's geotechnical and geological attributes, including the distinct characteristics of its members such as the Zutphen and Ockenburg Members, and the influence of weak zones. The dataset revealed significant heterogeneity in the Kreftenheye Formation, particularly in grain size distribution and cone resistance values, reflecting its complex depositional history.

The general analysis of the Kreftenheye Formation showed a clear alignment between the geological history of the deposits and the observed phenomena in the data. This alignment confirms that the geological context is well-represented in the geotechnical measurements.

A major contribution of this thesis is the detailed examination of spatial trends and differences between Areas A and B within the Kreftenheye Formation. Shaped by distinct climatic and depositional conditions, these areas display different geotechnical properties that are crucial for accurate ground modeling and foundation design. The findings suggest that these areas should be modeled separately to capture their unique characteristics effectively.

The study also underscores the importance of integrating geological and geotechnical data. Discrepancies between CPT data and borehole observations highlight the need to consider geological context in interpreting CPT results. For example, the influence of the Wijchen Bed on CPT measurements and the presence of weak zones within the Kreftenheye Formation illustrate the complexity of subsurface conditions and the necessity of combining geological surveys with geotechnical data for a comprehensive analysis.

The application of the Boulanger & DeJong (2018) filter method improved data interpretation by removing transition zones, though further refinement and field calibration of this method are recommended to enhance its accuracy and reliability.

In summary, this thesis demonstrates the value of integrating diverse data types to deepen our understanding of the Kreftenheye Formation. The analysis highlights the formation's geotechnical and geological complexities and the importance of addressing these complexities to improve geotechnical assessments. This approach contributes to the safe and sustainable develop-

ment of infrastructure in the Netherlands.

Future research should focus on several key areas to enhance our understanding of the Kreftenheye Formation. First, detailed, more localized studies on the distribution of weak layers within the Kreftenheye deposit could offer valuable insights and improve modeling accuracy, which is crucial for effective subsurface management. Additionally, further investigation into the differences between Area A and Area B could involve analyzing variations in grain shape, which may provide a more comprehensive understanding of their distinct geotechnical properties. Finally, additional research on the Ockenburg Member, particularly regarding its calcium carbonate content, is recommended to explain the factors contributing to the high cone resistances observed. These studies will advance our ability to predict and manage subsurface conditions, supporting more precise and reliable geotechnical assessments and foundation development.

Bibliography

Ahmadi, M. M. & Robertson, P. K. (2005). Thin-layer effects on the CPT q_c measurement. *Canadian Geotechnical Journal*, 42(5), 1302–1317.

Amorosi, A. & Marchi, N. (1999). High-resolution sequence stratigraphy from piezocone tests: an example from the Late Quaternary deposits of the southeastern Po Plain. *Sedimentary Geology*, 128(1), 67–81.

Berendsen, H. & Stouthamer, E. (2000). Late Weichselian and Holocene palaeogeography of the Rhine–Meuse delta, the Netherlands. *Palaeogeography, Palaeoclimatology, Palaeoecology*, 161(3-4), 311–335.

Bosch, J. H. A., Harting, R., & Gunnink, J. T. (2014). *Lithologische karakterisering van de GeoTOP van Noord-Nederland (Hoofdgebied 5)*. TNO-rapport TNO 2014 R10680, TNO.

Boskalis (2024). Project Meanderende Maas. `https://nederland.boskalis.com/projecten/project-meanderende-maas`. Accessed: 2024-04-30.

Boulanger, R. & DeJong, J. (2018). Inverse filtering procedure to correct cone penetration data for thin-layer and transition effects. In *Cone penetration testing 2018* (pp. 25–44). CRC Press.

Boulanger, R. & Idriss, I. (2014). *CPT and SPT Based Liquefaction Triggering Procedures*. Davis, CA: Center for Geotechnical Modeling, Department of Civil and Environmental Engineering, University of California, Davis.

Buma, J. T., de Heer, E., Bus, S. A. R., Harting, R., & Booltink, W. (2024). *TopIntegraal, het boor- en meetprogramma van de ondiepe ondergrond van Nederland - Deelrapport 1. Meetgegevens en kentallen verzadigde doorlatendheid, versie 1.0*. TNO-rapport TNO 2023 R10561, TNO - Geologische Dienst Nederland, Utrecht.

Busschers, F. (2008). *Unravelling the Rhine: Response of a fluvial system to climate change, sea-level oscillation and glaciation*. Phd-thesis - research and graduation internal, Vrije Universiteit Amsterdam.

Busschers, F. S., Kasse, C., van Balen, R. T., Vandenberghe, J., Cohen, K. M., Weerts, H. J. T., Wallinga, J., Johns, C., Cleveringa, P., & Bunnik, F. P. M. (2007). Late Pleistocene Evolution of the Rhine-Meuse System in the Southern North Sea Basin: Imprints of Climate Change, Sea-Level Oscillation, and Glacio-Isostacy. *Quaternary Science Reviews*, 26, 25–28.

Busschers, F. S., Weerts, H. J. T., Wallinga, J., Cleveringa, P., Kasse, C., de Wolf, H., & Cohen, K. M. (2005). Sedimentary Architecture and Optical Dating of Middle and Late Pleistocene Rhine-Meuse Deposits - Fluvial Response to Climate Change, Sea-Level Fluctuation and Glaciation. *Netherlands Journal of Geosciences - Geologie en Mijnbouw*, 84(1), 25–41.

Campanella, R. G., Gillespie, D., & Robertson, P. (1982). Pore Pressures During Cone Penetration Testing. In *Proceedings of the European Symposium on Penetration Testing (ESOPT 2)* (pp. 507–512). Amsterdam, Netherlands: A.A. Balkema. Bibliography includes 5 references; Illustrated.

Chai, F. & Tehrani, F. S. (2022). Effect of Weak Zones on Foundation Pile Response. In *Proceedings of the International Symposium on Geotechnical Engineering* (pp. Page numbers, if available). Location of the symposium, if available: Publisher, if available. Details about the symposium, such as date or any additional notes.

Cox, M. R. & Budhu, M. (2008). A practical approach to grain shape quantification. *Engineering Geology*, 96(1), 1–16.

de Gijt, J. G., Brassinga, H. E., & Roubos, A. A. (2019). Some learning cases in the Port of Rotterdam. *IOP Conference Series: Materials Science and Engineering*, 615(1), 012052.

de Lange, D. A. (2018). *CPT in Thinly Layered Soils: Validation Tests and Analysis for Multi Thin Layer Correction*. Technical Report 120, Nederlandse Aardolie Maatschappij.

Duffy, K., Gavin, K., Korff, M., de Lange, D., & Roubos, A. (2024). Influence of Installation Method on the Axial Capacity of Piles in Very Dense Sand. *Journal of Geotechnical and Geoenvironmental Engineering*, 150(6), 04024043.

Ecopedia (2024). Meander. `https://www.ecopedia.be/encyclopedie/meander`. Accessed: [Access Date].

EOS (2023). Natural Floodplains Are Quickly Vanishing. `https://eos.org/articles/natural-floodplains-are-quickly-vanishing`. Accessed: [Access Date].

Eshel, G., Levy, G. J., Mingelgrin, U., & Singer, M. J. (2004). Critical Evaluation of the Use of Laser Diffraction for Particle-Size Distribution Analysis. *Soil Science Society of America Journal*, 68(3), 736–743.

FUGRO Ingenieursbureau B.V. (2010). *Geotechnisch Onderzoek betreffende Plan de Geest te Beek Ubbergen*. Technical report, FUGRO Ingenieursbureau B.V., Kermisland 110, Postbus 5251, 6802 EG Arnhem, Netherlands. Opdrachtnummer: 6009-0361-000. Opdrachtgever: Sirius Vastgoedontwikkeling BV, Oranjesingel 65, 6511 NR Nijmegen. Datum grondonderzoek: 4 november 2009 tot 18 februari 2010. Projectleider: drs. O. Duizendstra.

Fukue, M., Nakamura, T., & Kato, Y. (1999). Cementation of Soils Due to Calcium Carbonate. *Soils and Foundations*, 39(6), 55–64.

Gebiedsontwikkeling.nu (2023). Het riviersysteem kraakt in de voegen en is aan revisie toe. `https://www.gebiedsontwikkeling.nu/artikelen/`

het-riviersysteem-kraakt-in-de-voegen-en-is-aan-revisie-toe/. Accessed: 2024-07-29.

Geographic, N. (2024). Marsh. https://education.nationalgeographic.org/resource/marsh/. Accessed: [Access Date].

Harting, R., Buma, J., & van Leer, M. (2023). Hydraulic conductivity measurements of aquitard sediments in the Netherlands. Mendeley Data, V1.

Koster, K., De Lange, G., Harting, R., de Heer, E., & Middelkoop, H. (2018). Characterizing void ratio and compressibility of Holocene peat with CPT for assessing coastal–deltaic subsidence. *Quarterly Journal of Engineering Geology and Hydrogeology*, 51(2), 210–218.

Krumbein, W. C. (1941). Measurement and geological significance of shape and roundness of sedimentary particles. *Journal of Sedimentary Research*, 11(2), 64–72.

Lafuerza, S., Canals, M., Casamor, J., & Devincenzi, J. (2005). Characterization of deltaic sediment bodies based on in situ CPT/CPTU profiles: A case study on the Llobregat delta plain, Barcelona, Spain. *Marine Geology*, 222-223, 497–510. Mediterranean Prodelta Systems.

Lambe, T. W. & Whitman, R. V. (1991). *Soil Mechanics*. New York: Wiley.

Lunne T., Powell J.J.M., . R. P. (1997). *Cone Penetration Testing in Geotechnical Practice (1st ed.)*. CRC Press.

Mayne, P. W. (2017). Stress History of Soils from Cone Penetration Tests. *Soils and Rocks*, 40(2), 203–218.

Meanderende Maas (2024). Meanderende Maas - Project Information. https://www.meanderendemaas.nl/. Accessed: 2024-07-30.

Natuurkennis (2024). Factsheet Kwelgeulen. https://www.natuurkennis.nl/Uploaded_files/Publicaties/factsheet-kwelgeulen-def.1c1734.pdf. Accessed: [Access Date].

NEN-EN-ISO (2021). Geotechnical investigation and testing - Sampling methods and groundwater measurements - Part 1: Technical principles for the sampling of soil, rock and groundwater. Definitive — 142 pages.

Netherlands Standardization Institute (2012). Nen-en-iso 22476-1:2012 en geotechnical investigation and testing - field testing - part 1: Electrical cone and piezocone penetration test.

Netherlands Standardization Institute (2020). Nen-en-iso 14688-1:2019+nen 8990:2020 nl: Geotechnical investigation and testing - identification and classification of soil - part 1: Identification and description.

Ngan-Tillard, D. J. M., Venmans, A. A. M., & Slob, E. (2010). Total engineering geology approach applied to motorway construction and widening in the Netherlands: Part I: A pragmatic approach. *Engineering Geology*, 114(3-4), 3–4.

Nichols, G. (2009). *Sedimentology and stratigraphy*. John Wiley & Sons.

Onyejekwe, S., Kang, X., & Ge, L. (2016). Evaluation of the scale of fluctuation of geotechnical parameters by autocorrelation function and semivariogram function. *Engineering Geology*, 214, 43–49.

Panayiotopoulos, K. P. (1989). Packing of sands—a review. *Soil and Tillage Research*, 13(2), 101–121.

Peeters, J., Busschers, F. S., & Stouthamer, E. (2015). Fluvial Evolution of the Rhine during the Last Interglacial-Glacial Cycle in the Southern North Sea Basin: A Review and Look Forward. *Quaternary International*, 357, 176–188.

Peeters, J., Busschers, F. S., & Stouthamer, E. (2020). Fluvial evolution of the Rhine during the last interglacial-glacial cycle in the southern North Sea basin: A review and look forward. *Quaternary Science Reviews*, 237, 106306.

Pettijohn, F. J. (1987). *Sand and Sandstone*. Springer, latest edition edition.

Peuchen, J., van Kesteren, W., Vandeweijer, V., Carpentier, S., & van Erp, F. (2022). Upscaling 1,500,000 Synthetic CPTs to Voxel CPT Models of Offshore Sites. In *Proceedings of the Conference* (pp. 641–645). Bologna, Italy: CRC Press.

Robertson, P. (1990). Soil classification using the cone penetration test. *Canadian Geotechnical Journal*, 27(1), 151–158.

Robertson, P. (2009). Interpretation of cone penetration tests – a unified approach. *Canadian Geotechnical Journal*, 46(11), 1337–1355.

Robertson, P. & Cabal, K. (2014). *Guide to Cone Penetration Testing for Geotechnical Engineering*. Gregg Drilling & Testing, Inc., 6th edition.

Robertson, P. K. (2016). Cone penetration test (CPT)-based soil behaviour type (SBT) classification system—an update. *Canadian Geotechnical Journal*, 53(12), 1910–1927.

Roubos, A. (2019). *Enhancing Reliability-Based Assessments of Quay Walls*. Ph.d. thesis, Delft University of Technology, Delft, the Netherlands.

Schiltz, M. (2020). On the use of CPTs in stratigraphy: recent observations and some illustrative cases. *The Neogene Stratigraphy of Northern Belgium*, 23(3-4). Open Access.

Schneider, J., Randolph, M., Mayne, P. W., & Ramsey, N. R. (2008). Analysis of Factors Influencing Soil Classification Using Normalized Piezocone Tip Resistance and Pore Pressure Parameters. *Journal of Geotechnical and Geoenvironmental Engineering*, 134(11), 1569–1586.

Schokker, J. & Koster, E. A. (2004). Sedimentology and Facies Distribution of Pleistocene Cold-climate Aeolian and Fluvial Deposits in the Roer Valley Graben (Southeastern Netherlands). *Permafrost and Periglacial Processes*, 15, 1–20.

Science, L. (2018). Greenland Is Melting Fast. `https://www.livescience.com/64243-greenland-is-melting-fast.html`. Accessed: [Access Date].

SIKB (2022). Plaatsen van handboringen en peilbuizen, maken van boorbeschrijvingen en nemen van grondmonsters: Installation of manual drills and monitoring wells, drawing up drilling descriptions and taking soil samples. Protocol 2001.

Tehrani, F. S., Arshad, M. I., Prezzi, M., & Salgado, R. (2018). Physical Modeling of Cone Penetration in Layered Sand. *Journal of Geotechnical and Geoenvironmental Engineering*, 144(1), 04017101.

TNO-GSN (2024). Online portal for subsurface information of the Netherlands. `www.dinoloket.nl/en`. Accessed: 2024-06-01.

Treviranus, I. (2013). Introduction to Laser Diffraction for Particle Size Analysis. `https://www.youtube.com/watch?v=ZFbs-sXF7Ss`. Accessed: 2024-07-31.

Ulusoy, U. (2019). Quantifying of particle shape differences of differently milled barite using a novel technique: Dynamic image analysis. *Materialia*, 8, 100434.

Van den Berg, P. (1994). *Analysis of Soil Penetration*. PhD thesis, Delft University of Technology, Delft, The Netherlands.

van den Berg, P. (1996). An Eulerian Finite Element Model for Penetration in Layered Soil. *International Journal for Numerical and Analytical Methods in Geomechanics*, 20(12), 865–886.

Vanneste, M., Sauvin, G., Dujardin, J. R., Forsberg, C. F., Klinkvort, R. T., Forsberg, C. S., & Hansen, R. C. (2022). Data-Driven Ground Models: The Road to Fully-Integrated Site Characterization and Design. In D. V. K. Huynh, A. M. Tang, D. H. Doan, & P. Watson (Eds.), *Proceedings of the 2nd Vietnam Symposium on Advances in Offshore Engineering* (pp. 3–21). Singapore: Springer.

Verbraeck, A. (1983). Sedimentation in the Mid-Netherlands River Area during the Late Weichselian. *Geologie en Mijnbouw*, 62, 487–491.

Vernes, R. W., Bosch, A. J., Harting, R., de Heer, E., & Griffioen, J. (2010). Towards a physical and chemical characterization of the shallow subsurface of the Netherlands. In *First International Conference on Frontiers in Shallow Subsurface Technology*: European Association of Geoscientists & Engineers. cp-150-00020.

Wong, T., Batjes, D., & de Jager, J. (2007). *Geology of the Netherlands*. Amsterdam: Royal Netherlands Academy of Arts and Sciences.

Youd, T. L. & Idriss, I. M. (2001). Liquefaction Resistance of Soils: Summary Report from the 1996 NCEER and 1998 NCEER/NSF Workshops on Evaluation of Liquefaction Resistance of Soils. *Journal of Geotechnical and Geoenvironmental Engineering*, 127(4), 297–313.

Zhang, S., Liu, W., & Granata, G. (2018). Effects of Grain Size Gradation on the Porosity of Packed Heap Leach Beds. *Hydrometallurgy*, 179, 238–244.